Supporting Information

Supramolecular Method Enabling Effective Through-Space Charge Transfer in Thermally Activated Delayed Fluorescence Materials with Pure Orange Emission

S1. Materials and Characterization

Materials

Cyclic peptide (CP-NH_2) with a sequence of cyclo-(L-Lys-D-Leu-L-Trp-D-Leu-L-Trp-D-Leu-L-Trp-D-Leu-) was synthesized previously within the group.[1] *O*-(7-azabenzotriazol-1-yl)-*N*,*N*,*N*',*N*'-tetramethyl uronium hexafluorophosphate (HATU), *N*-methylmorpholine (NMM), 4-cyano-4-[(ethylsulfanylthiocarbonyl)sulfanyl]pentanoic acid (CTA-CN), and other chemicals were purchased from several suppliers, including Bidepharm, J&K, and Sigma-Aldrich. Solvents were purchased from several local suppliers, including General-Reagent, and J&K.

Characterization

Nuclear Magnetic Resonance Spectroscopy (NMR): ^{1}H NMR spectra were measured using a Bruker Avance III HD 400 MHz NMR spectrometer with chloroform-*d* ($CDCl_3$) or dimethyl sulfoxide-d_6 (DMSO-d_6) as the solvent. The residual solvent peaks were used as internal references.

Liquid Chromatography-Mass Spectrometry (LC-MS): LC-MS analysis was conducted using a WATERS H-Class/QDa Mass Spectrometer coupled with a WATERS ACQUITY UPLC to characterize the chemicals in positive ion mode. Water and acetonitrile were used as mobile phase A and B, respectively. All solvents contained 0.1 % (v/v) formic acid. Samples were dissolved in mobile phase B with a final concentration of 0.1 mg mL^{-1} and the injection volume was 2 μL.

Ultraviolet–Visible (UV–Vis) Absorption Spectroscopy: UV–vis absorption spectra were measured using a SHIMADZU UV-2600i UV–vis spectrometer. Unless otherwise stated, the path length of the cuvette was 10 mm.

Steady State Fluorescence Spectroscopy: Fluorescence emission spectra were measured using either an Edinburgh Instruments FLS1000 photoluminescence spectrometer or a HITACHI F-4700 fluorescence spectrometer.

Time-resolved Fluorescence Spectroscopy: Fluorescence lifetime measurements were performed using an Edinburgh Instruments FLS1000 photoluminescence spectrometer, equipped with several Pulsed Lasers - EPL Series.

Absolute Photoluminescence Quantum Yield (PLQY): PLQY was measured using an Edinburgh Instruments FLS1000 photoluminescence spectrometer equipped with an Edinburgh Integrating Sphere Module.

Small Angle Neutron Scattering (SANS): SANS was carried out at the SANS instrument in China Spallation Neutron Source (CSNS). The sample to detector distance was set to 4 m, with a wavelength band from 1 Å to 9.8 Å, yielding a q-range of 0.005 $Å^{-1}$ – 0.9^{-1} $Å^{-1}$. Samples with deuterated solvent were loaded in the Hellma quartz cells with 2 mm light path and measured at room temperature. The scattering profiles of the samples have been calibrated to absolute scaling with sample transmission and a secondary standard sample (Bates-poly) provided by the beamline. The corresponding background contributions including solvent, empty cell as well as empty beam data were also collected and properly subtracted before data analysis.

Cyclic voltammetry (CV): The CV curves was obtained using a CHI 660E Electrochemical Workstation purchased from Shanghai Chenhua Instrumental Co., Ltd. China, and the glassy carbon disk was the working electrode, the Pt wire is a counter electrode, the Ag/Ag^{+} electrode is the reference electrode. The potential scan rate is 100 mV s^{-1} with 0.1 mol L^{-1} tetrabutylammonium phosphorus hexafluoride (n-Bu_4NPF_6) in solution in MeCN as an electrolyte.

Gel Permeation Chromatography (GPC): Molecular weights of the Ac/NAI polymers were determined using high temperature GPC based on Agilent Technologies 1260 infinity II system. 1,2,4-Trichlorobenzene (1,2,4-TCB) was used as the eluent with a flow rate of 1.0 mL min^{-1} at 150 °C. Molecular weights of the block copolymers containing *p*DMA were determined by GPC measurements on a Waters ACQUITY APC System equipped with a UV detector (Waters ACQUITY TUV) and 3 series connected chromatographic columns (ACQUITY APC XT 450, 200, 45, 4.6 × 150 mm). THF was used as the eluent with a flow rate of 0.5 mL min^{-1} at 40 °C.

S2. Characterization of TSCT TADF Polymers

Sample preparation: In a 5 mL vial, a precise amount of the as-synthesized TADF small molecule or polymer was accurately weighed. A specific volume of solvent was added to prepare a stock solution with a total monomer concentration of 20 mM. Appropriate shaking and heating were necessary to ensure complete dissolution. Unless otherwise stated, the stock solution was diluted to 500 μM for spectroscopy experiments.

Film preparation: 100 μL of polymer stock solution was drop-casted onto a quartz substrate, and then dried via natural air to form a thin, transparent film.

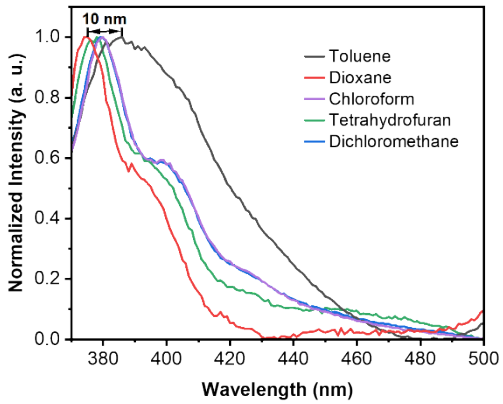

Figure S1. PL emission spectra of *p*(Ac-co-NAI) in different solvents showing solvatochromic effect of the LE peak.

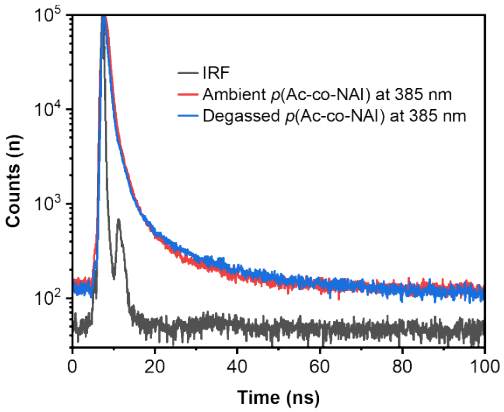

Figure S2. Time resolved fluorescence spectra of *p*(Ac-co-NAI) at 385 nm in ambient and degassed toluene solution.

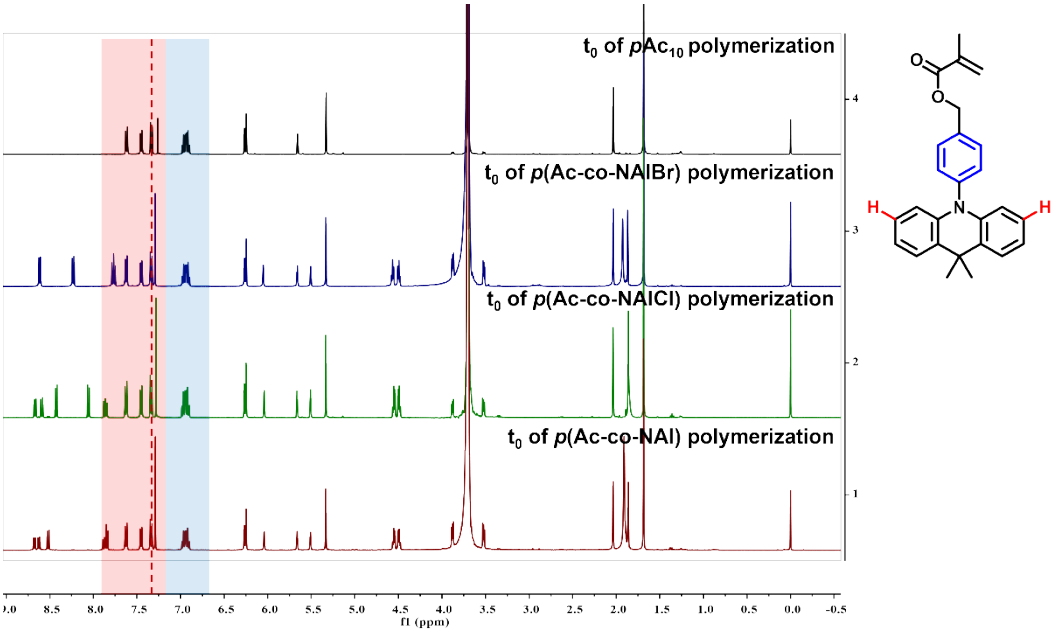

Figure S3. ^{1}H NMR (400 MHz, $CDCl_3$) spectra before the polymerization pAc_{10}, *p*(Ac-co-NAI), *p*(Ac-co-NAICl), and *p*(Ac-co-NAIBr).

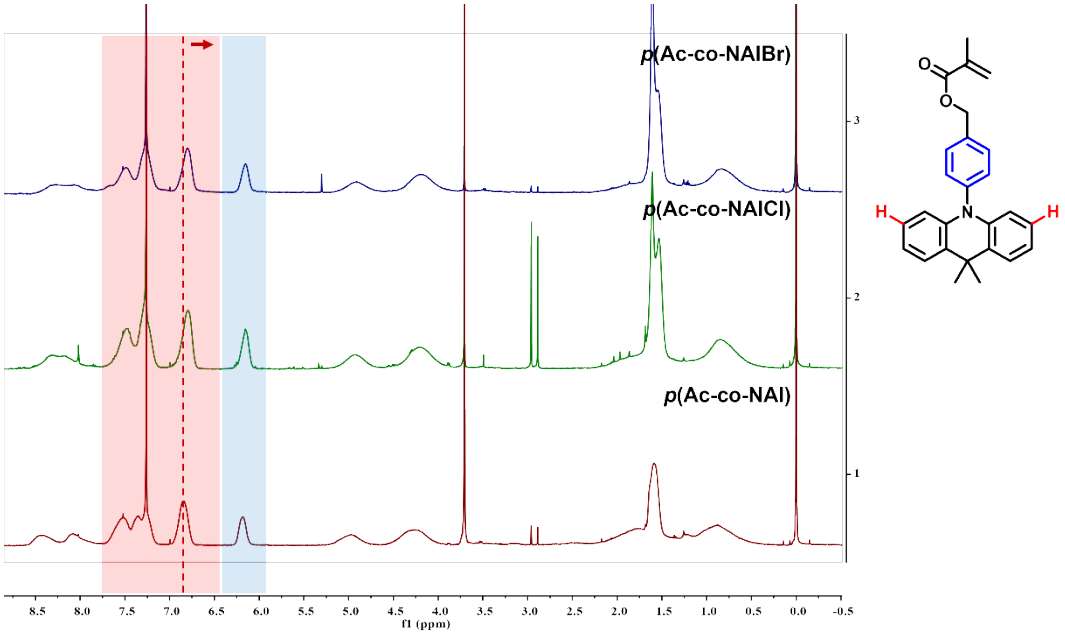

Figure S4. ^{1}H NMR (400 MHz, $CDCl_3$) spectra of *p*(Ac-co-NAI), *p*(Ac-co-NAICl), and *p*(Ac-co-NAIBr).

Table S1. Photophysical parameters of the TSCT-TADF polymers in toluene.

	λ_{PL} nm	*PLQY* %	τ_p ns	τ_d ns
Ac-co-NAI	405 610	2.17	24.0	1312.2
Ac-co-NAICl	407 635	1.64	13.4	738.5
Ac-co-NAIBr	407 650	0.94	5.0	735.0

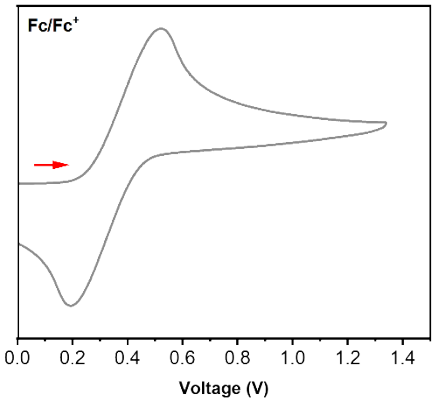

Figure S5. Voltammogram of the reversible reduction of a 1 mM Fc^+ solution to Fc.

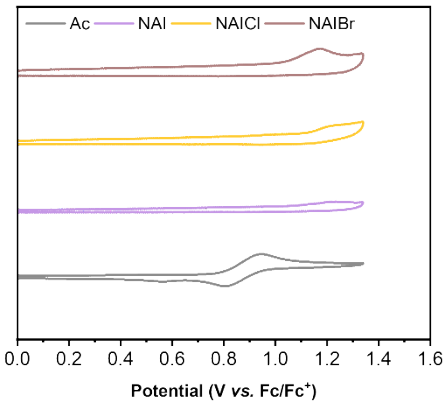

Figure S6. Cyclic voltammetry (CV) curves of donor and acceptors for TSCT-TADF polymers.

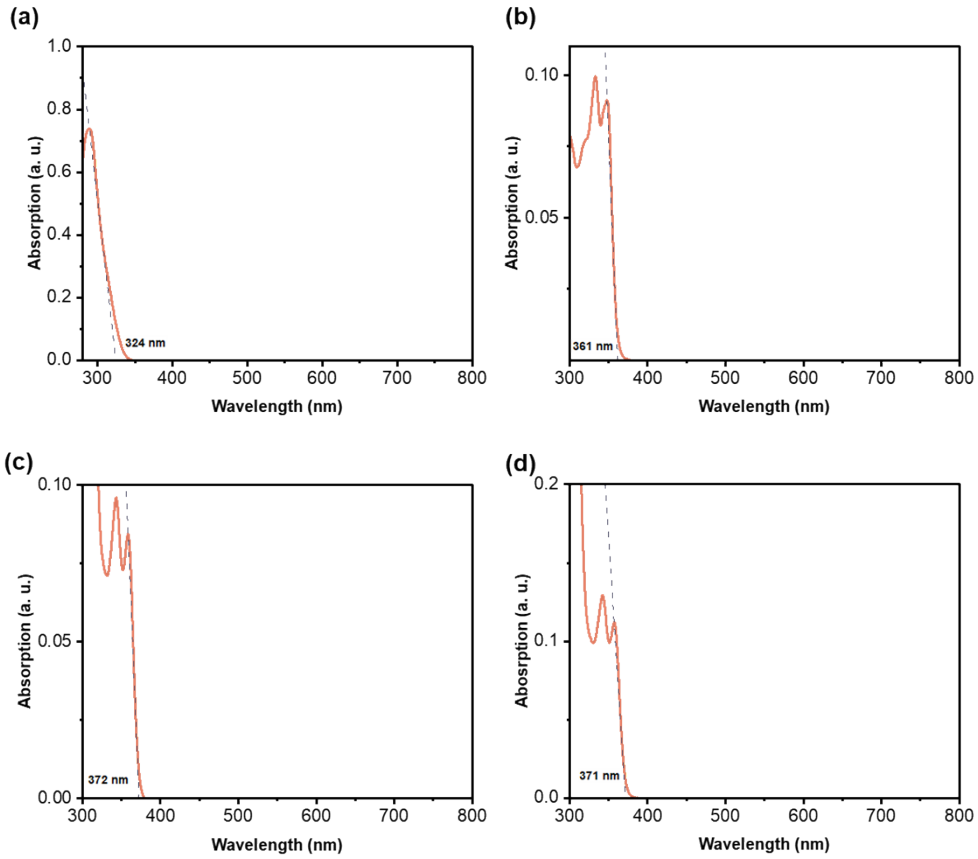

Figure S7. UV-Vis absorption spectra of (a) Ac (b) NAI (c) NAICl (d) NAIBr monomer showing absorption onset.

Table S2. UV-Vis absorption data and energy levels of donor and acceptors for TSCT-TADF polymers.

	λ_{max} (nm)	λ_{onset} (nm)	E_g (eV)	HOMO (eV)	LUMO (eV)
Ac	289	323	3.84	-5.27	-1.42
NAI	333, 348	361	3.43	-6.60	-3.17
NAICl	342, 357	371	3.34	-6.56	-3.23
NAIBr	343, 359	372	3.33	-6.63	-3.3

The HOMO and LUMO levels were calculated according to the equation: E_{HOMO}= -e[$E_{onset,\ ox}$ + 4.8 V], where $E_{onset,\ ox}$ is the onset of the oxidation waves, LUMO= HOMO + E_g, The optical gaps (E_g) obtained from UV-Vis absorption spectra as shown in Figure S7.

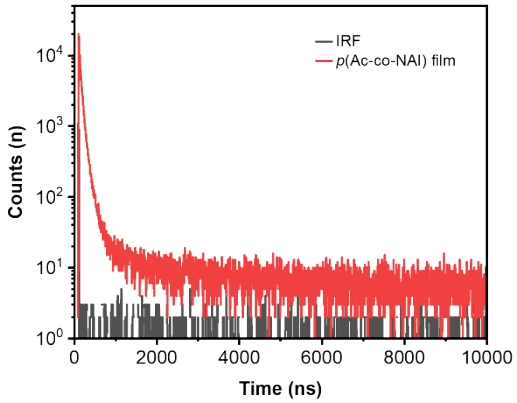

Figure S8. PL lifetime decay profile of *p*(Ac-co-NAI) film.

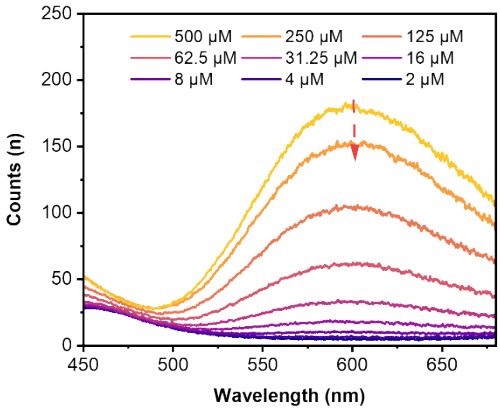

Figure S9. Concentration-dependent PL spectra of *p*(Ac-co-NAI) in toluene.

S3. Characterization of Supramolecular TSCT-TADF Systems

Sample preparation: The self-assembly of the supramolecular systems was realized by firstly mixing the components in a small amount of DMF, followed by the addition of DI water, resulting clear solutions with H_2O/DMF ratio of 95/5. In the case of SANS, deuterated solvents were used (i.e. DMSO-d_6 instead of DMF, D_2O instead of H_2O).

For the self-assembly of Supra [Ac-NAI]-I: 21 μL CP-*p*Ac-*b*-*p*DMA (4 mM, DMF), 42 μL CP-NAI (4 mM, DMF) and 37 μL DMF were premixed in a vial, then 1900 μL DI water was added to induce self-assembly. The solution was kept in the dark at room temperature before measurements.

For the self-assembly of *p*[Ac-co-NAI]-*b*-*p*DMA: 50 μL *p*[Ac-co-NAI]-*b*-*p*DMA (2 mM, DMF), and 50 μL DMF were premixed in a vial, then 1900 μL DI water was added to induce

self-assembly. The solution was kept in the dark at room temperature before measurements.

For the self-assembly of Supra [Ac-NAI]-II: 17 μL CP-*p*Ac-*b*-*p*DMA (4 mM, DMF), 17 μL CP-*p*[Ac-co-NAI]-*b*-*p*DMA (2 mM, DMF) and 66 μL DMF were premixed in a vial, then 1900 μL DI water was added to induced self-assembly. The solution was kept in the dark at room temperature before measurements.

For the self-assembly of supramolecular TAF system based on Supra [Ac-NAI]-II: 25 μL CP-*p*Ac-*b*-*p*DMA (2 mM, DMF), 25 μL CP-*p*[Ac-co-NAI]-*b*-*p*DMA (2 mM, DMF), 17 μL CP-Cy5.5 (1 mM, DMF) and 33 μL DMF were premixed in a vial, then 1900 μL DI water was were added to induce self-assembly. The solutions were kept in the dark at room temperature before measurements.

SasView software was used to fit the SANS data, using a core-shell cylinder model. In this case, the core corresponds to the cyclic peptide, and the shell is assumed to be solvated polymer. SLD values were calculated based on the molecular structure of the conjugate and solvent. The radius of the core value was fixed at 5 Å, representing the radius of the cyclic peptide itself. The fitting procedure was performed to minimize the reduced χ^2, which is normalized by the number of data points and the number of fitting parameters.

Table S3. Fitting parameters using a core-shell cylinder model with SasView software.

SAMPLE	Supra [Ac-NAI]-I	Supra [Ac-NAI]-II
Scale	0.774±0.022	0.131±0.036
Background*	0.001	0.004
sld_core*	2.03	2.03
sld_shell	6.263±0.002	6.020±0.055
sld_solvent*	6.376	6.376
Radius* / Å	5	5
Thickness / Å	56.7±0.2	45.7±0.8
Length / Å	2000*	230.6±5.1
Distri. of thickness*	0.35	0.33
Reduced χ^2	91.9	1.3

Parameters marked with * were held constant throughout the fitting procedure, mean ± SD.

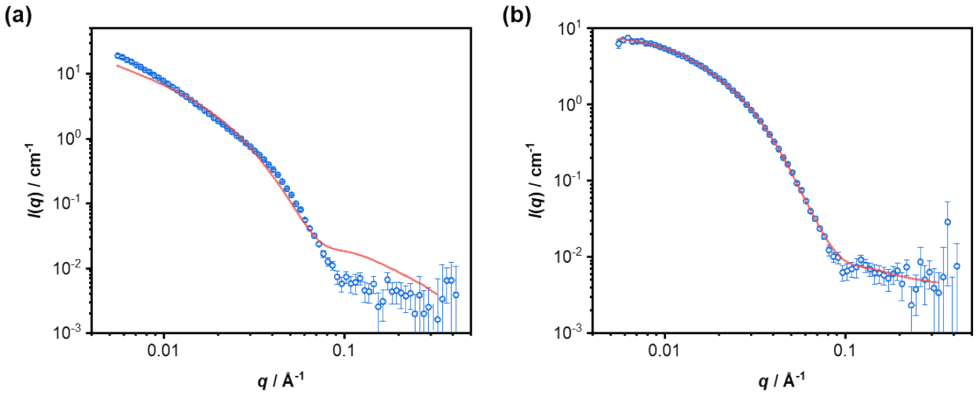

Figure S10. SANS scattering data and fitting to a core-shell cylinder model of Supra [Ac-NAI]-I (a) and Supra [Ac-NAI]-II (b).

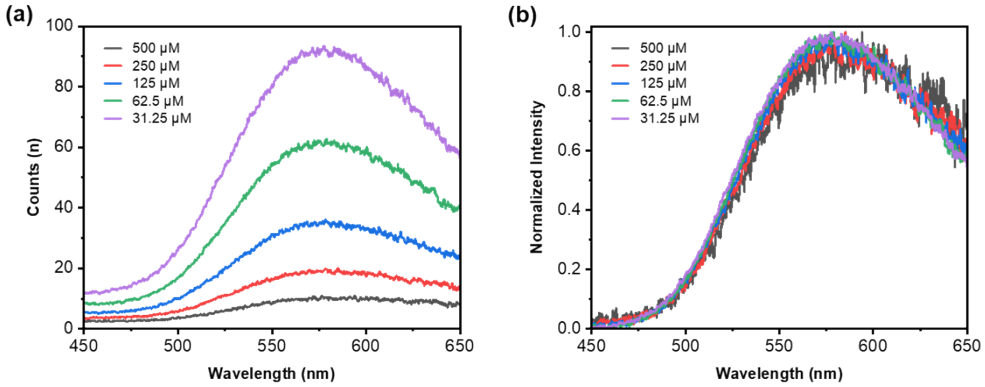

Figure S11. PL spectra (a) and normalized PL spectra (b) of Supra [Ac-NAI]-II at various concentrations.

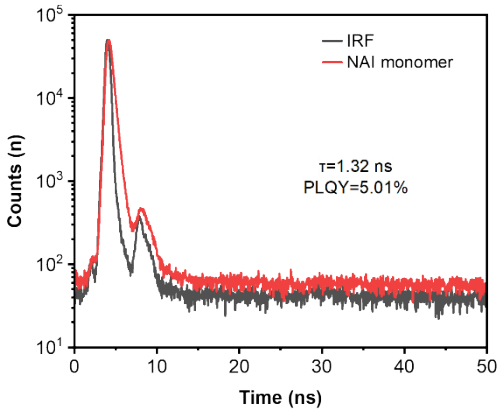

Figure S12. PL lifetime decay profile of NAI monomer.

Table S4. Physical data and kinetic parameters of the supramolecular TSCT-TADF systems in aqueous phase (TADF constants were calculated according to previous reports[2, 3]).

	λ_{PL} nm	*PLQY* %	τ_p ns	τ_d ns	k_r 10^5 s^{-1}	k_{nr} 10^7 s^{-1}	k_{ISC} 10^6 s^{-1}	k_{RISC} 10^6 s^{-1}
Supra [Ac-NAI]-I	405 575	0.39	20.9	138.9	1.62	4.13	6.39	1.28
***p*[Ac-co-NAI]-*b*-*p*DMA**	397 599	0.46	16.8	71.8	1.97	4.26	16.7	7.61
Supra [Ac-NAI]-II	575	1.24	43.8	358.4	2.70	2.15	1.03	13.95

Determination of singlet oxygen generation: The production of singlet oxygen ($^1O_2$) in solution was monitored using 9, 10-anthracenediyl bis(methylene) dimalonic acid (ABDA) as a probe. *p*Ac-*b*-*p*DMA, *p*[Ac-co-NAI]-*b*-*p*DMA, or Supra [Ac-NAI]-II was each mixed with ABDA (100 μM) in PBS. The reaction mixture was placed in a quartz cuvette, and the absorbance of ABDA was measured by UV-Vis spectroscopy at 298 K after continuous irradiation for different time intervals using a Xe lamp (350 nm ± 3 nm).

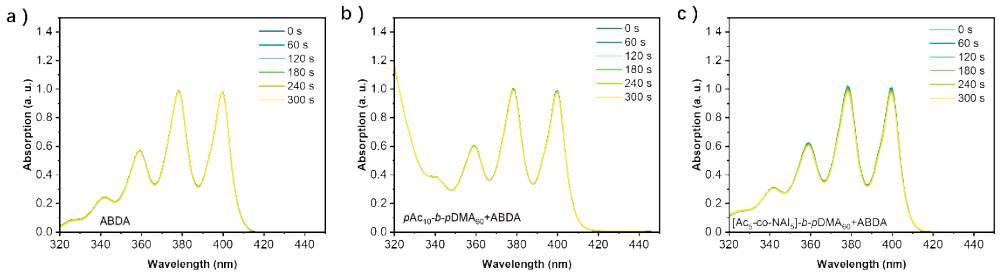

Figure S13. UV−Vis absorption spectra of a) ABDA b) $p\text{Ac}_{10}$-*b*-$p\text{DMA}_{60}$/ABDA c) $p[\text{Ac}_5\text{-co-NAI}_5]$-*b*-$p\text{DMA}_{60}$/ABDA under continuous irradiation.

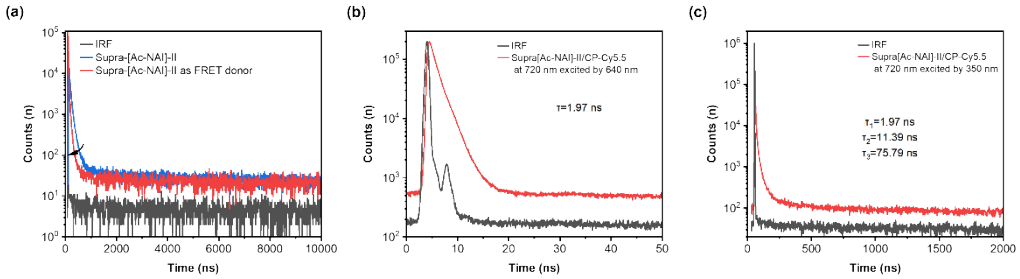

Figure S14. Time resolved fluorescence spectra of (a) Supra [Ac-NAI]-II at 600 nm with/without FRET acceptor; (b) Supramolecular TAF system at 720 nm excited by 640 nm; (c) Supramolecular TAF system at 720 nm excited by 350 nm.

S4. Synthetic protocols

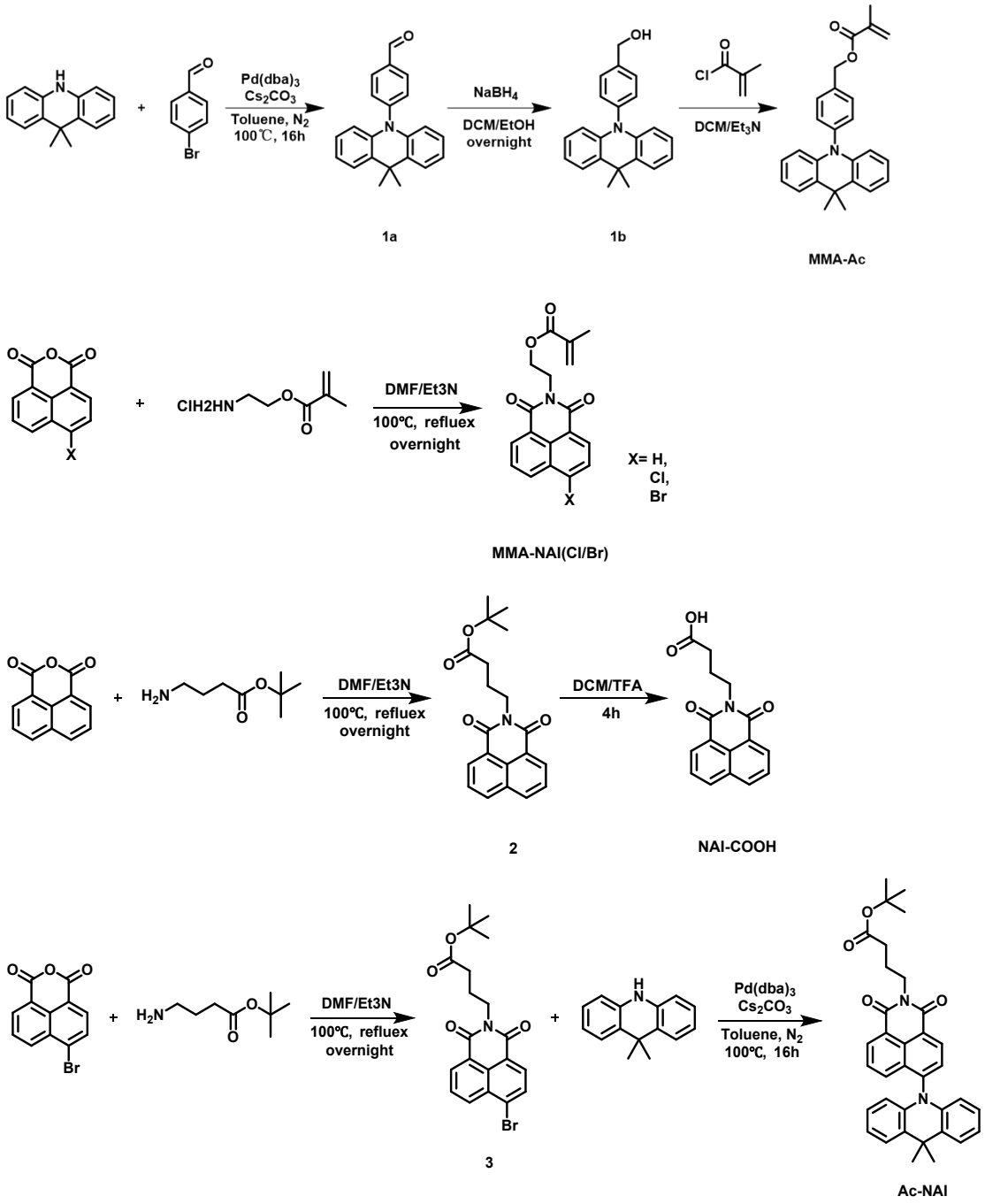

Scheme S1. Synthetic routines of small molecules.

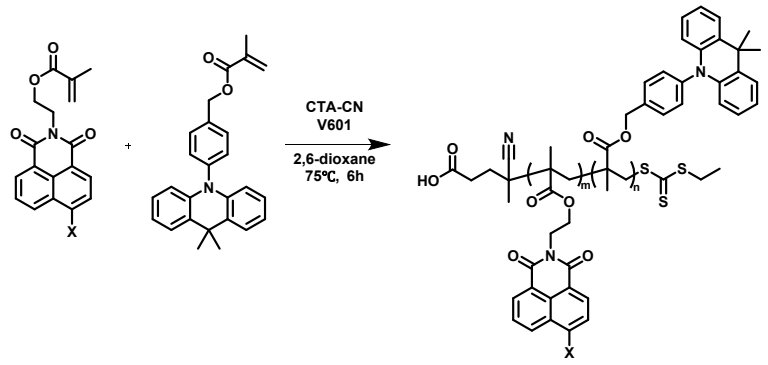

X	m	n	Polymer
H	5	5	*p*(Ac_5-co-NAI_5)
H	10	50	*p*(Ac_{50}-co-NAI_{10})
H	20	40	*p*(Ac_{40}-co-NAI_{20})
H	30	30	*p*(Ac_{30}-co-NAI_{30})
H	40	20	*p*(Ac_{20}-co-NAI_{40})
H	50	10	*p*(Ac_{10}-co-NAI_{50})
Cl	30	30	*p*(Ac_{30}-co-$NAICl_{30}$)
Br	30	30	*p*(Ac_{30}-co-$NAIBr_{30}$)

Scheme S2. Synthetic routine of the TSCT-TADF copolymers.

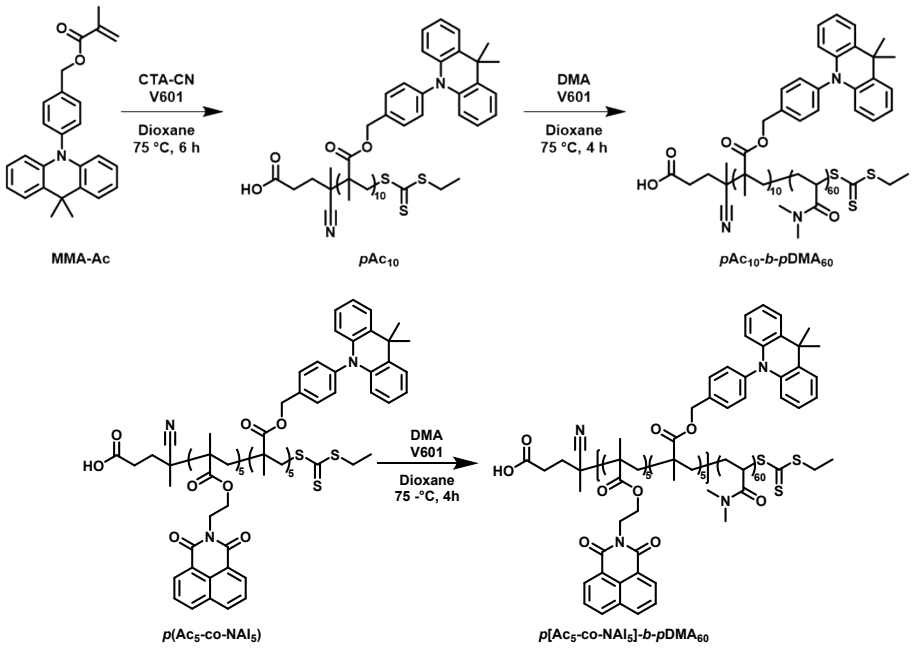

Scheme S3. Synthetic routine of amphiphilic polymers.

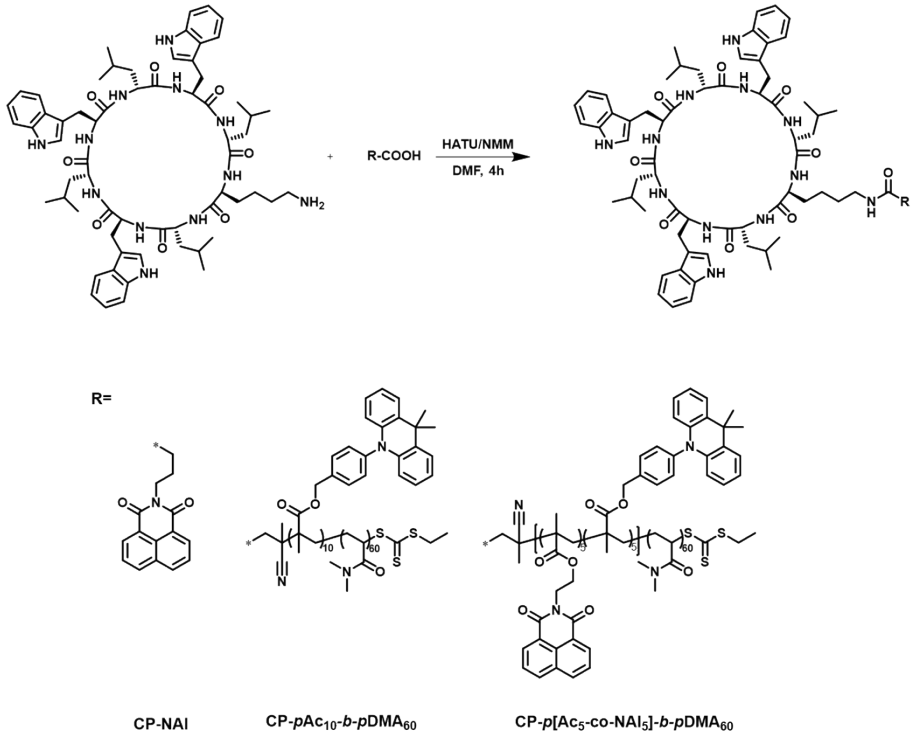

Scheme S4. Synthetic routine of cyclic peptide-based supramolecular units.

Synthetic procedure of 4-(9, 9-dimethylacridin-10(9H) -yl) benzaldehyde (1a)

1a was synthesized following a modified literature procedure.[4] In a 100 mL round-bottom flask, 9,9-dimethyl-9,10-dihydroacridine (1.25 g, 5.95 mmol), 4-bromobenzaldehyde (1.00 g, 5.40 mmol), tris(dibenzylideneacetone)dipalladium (247 mg, 0.27 mmol), 1,1'-bis(diphenylphosphino)ferrocene (299 mg, 0.54 mmol), cesium carbonate (5.30 g, 15.20 mmol), and dry toluene (30 mL) were combined and stirred at 100 °C under an argon atmosphere for 16 h. After the reaction was complete, the solvent was removed under reduced pressure. The resulting mixture was extracted with dichloromethane (3 × 50 mL) and washed successively with water and brine. The organic layer was dried over anhydrous sodium sulphate, and the solvent was evaporated. The crude product was purified by column chromatography using a petroleum ether and dichloromethane mixture (3:1, v/v) as the eluent, yielding **1a** as a pale-yellow solid (1.35 g, 80%).

^{1}H NMR (400 MHz, $CDCl_3$) δ = 10.12 (s, 1H), 8.17–8.09 (dt, 2H), 7.58–7.50 (dt, 2H), 7.54–7.43 (dd, 2H), 7.05–6.93 (m, 4H), 6.37–6.28 (dd, 2H), 1.68 (s, 6H).

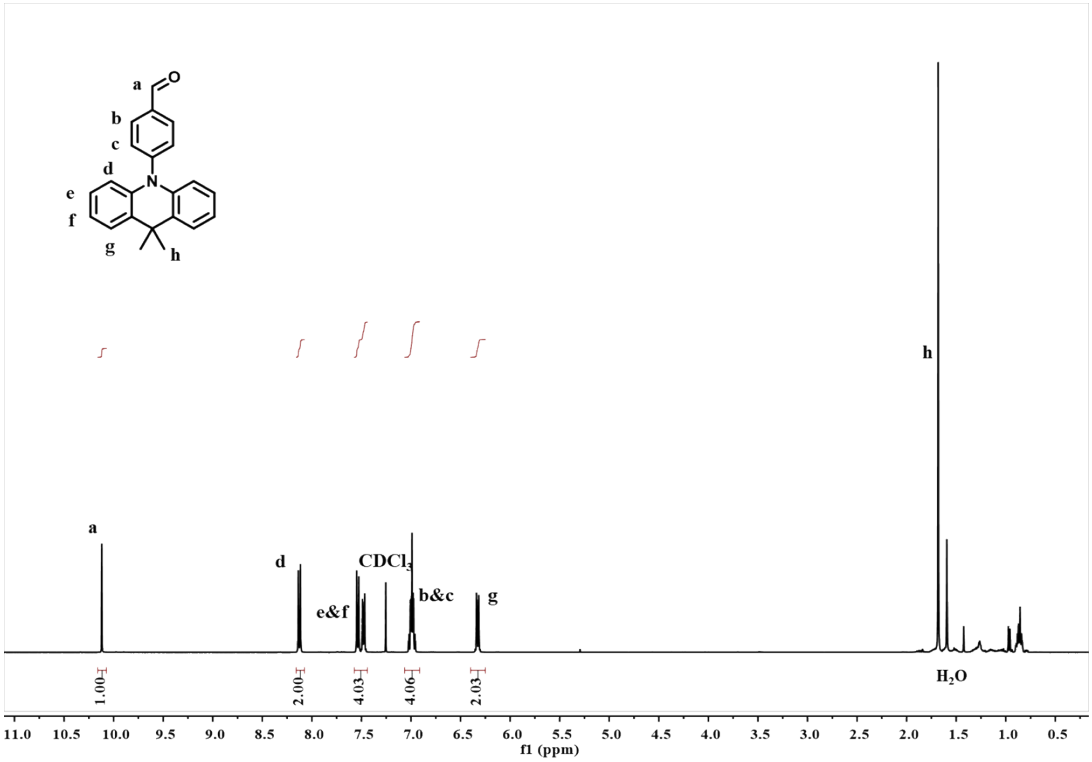

Figure S15. ^{1}H NMR (400 MHz, $CDCl_3$) spectrum of **1a**.

Synthesis procedure of (4-(9,9-dimethylacridin-10(9H)-yl)phenyl)methanol (1b)

1b was synthesized following a previously reported procedure.[5] To a solution of **1a** (626 mg, 2 mmol) in dichloromethane (20 mL) and ethanol (7 mL), sodium borohydride (114 mg, 3 mmol) was added. To reaction mixture was stirred at room temperature for 24 h. After completion, the reaction was quenched with 1 M ammonium chloride solution. The organic layer was separated, dried over anhydrous sodium sulphate, and concentrated under reduced pressure. The resulting residue was purified by column chromatography on silica gel using petroleum ether and dichloromethane (1:1, v/v) as the eluent, yielding **1b** as a white solid (580 mg, 92%).

^{1}H NMR (400 MHz, $CDCl_3$) δ = 7.66–7.60 (m, 2H), 7.45 (dd, 2H), 7.36–7.30 (m, 2H), 6.94 (m, 4H), 6.26 (dd, 2H), 4.84 (s, 2H), 1.69 (s, 6H).

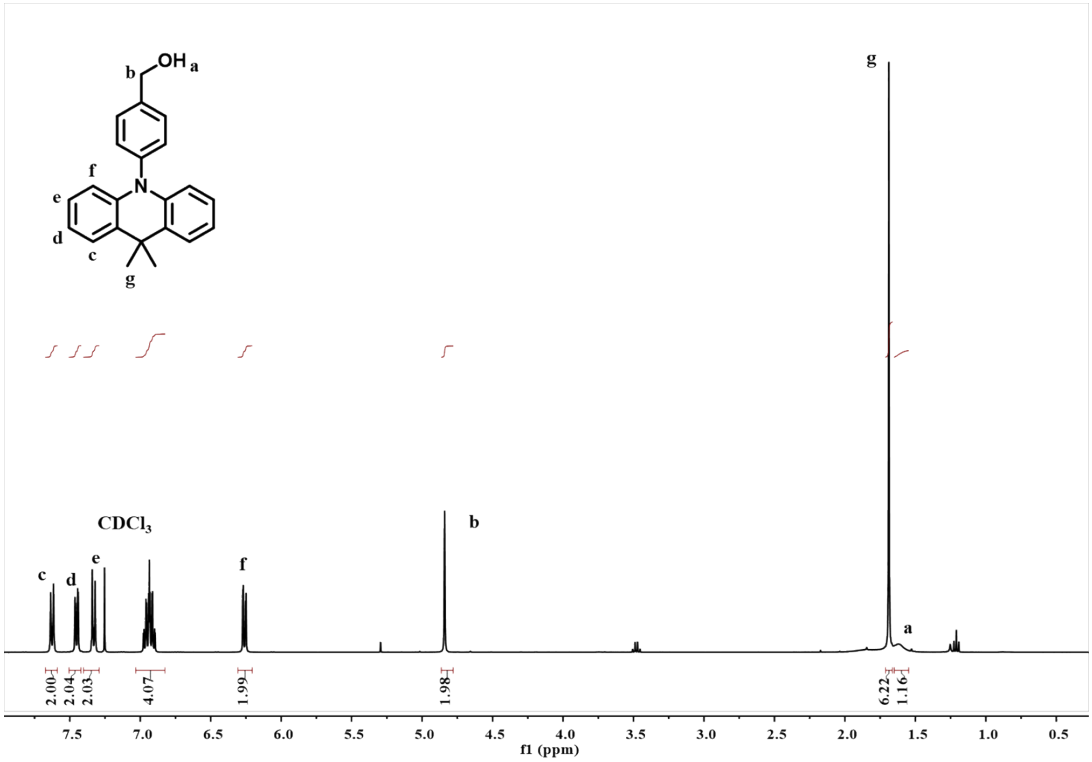

Figure S16. ^{1}H NMR (400 MHz, $CDCl_3$) spectrum of **1b**.

Synthesis procedure of MMA-Ac

MMA-Ac was synthesized following a previously reported procedure.[6] In a 50 mL round-bottom flask, **1b** (473 mg, 1.5 mmol) and triethylamine (313 μL, 2.25 mmol) were dissolved in dichloromethane (8 mL) under an argon atmosphere. The flash was cooled to 0 ℃ in an ice bath, and methacryloyl chloride (136 μL, 1.65 mmol) was added dropwise over 10 min. The mixture was then shielded from light with foil and stirred at room temperature for 24 h. After the reaction, the mixture was quenched with water and extracted with dichloromethane (3 × 30 mL). The organic layers were combined, dried over anhydrous sodium sulphate, and concentrated under reduced pressure. The residue was purified by column chromatography with petroleum ether and dichloromethane (1:2, v/v) as the eluent, yielding **1c** as a yellow solid (352 mg, 63%).

^{1}H NMR (400 MHz, $CDCl_3$) δ = 7.66 (d, 2H), 7.49 (d, 2H), 7.37 (d, 2H), 7.10 – 6.83 (m, 4H), 6.30 (s, 1H), 6.29 (s, 2H), 5.69 (s, 1H), 5.37 (s, 2H), 2.07 (s, 3H), 1.72 (s, 6H).

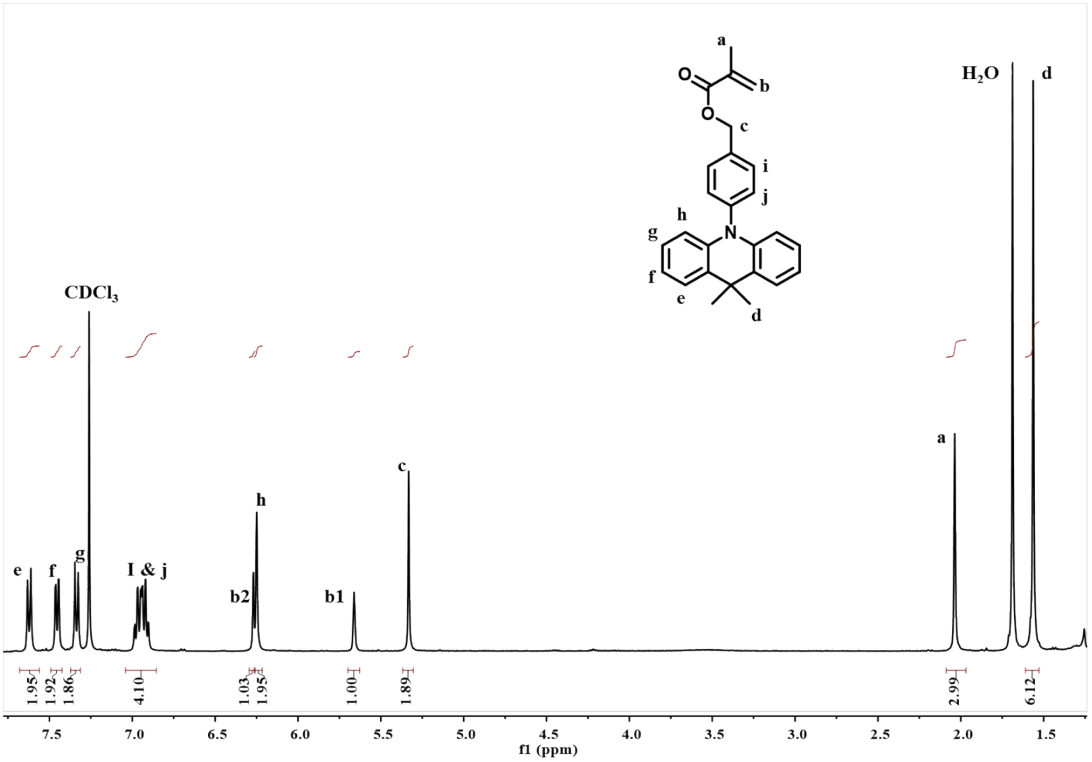

Figure S17. ^{1}H NMR (400 MHz, $CDCl_3$) spectrum of **MMA-Ac**.

Synthetic procedure of MMA-NAI

1,8-Naphthalic anhydride (1 g, 5.05 mmol) and 2-aminoethylmethacrylate hydrochloride(919 mg, 5.55 mmol) were dissolved in DMF (60 mL), followed by the addition of triethylamine (752 µL, 5.4 mmol). The mixture was stirred at 100 °C for 16 h. After cooling to room temperature, the reaction mixture was extracted with dichloromethane and water. The organic layers were combined, dried over anhydrous sodium sulphate, and the solvent was removed under reduced pressure. The residue was purified by column chromatography with petroleum ether and dichloromethane (5:1, v/v) as the eluent, yielding **MMA-NAI** as a pale-yellow solid (913 mg, 58%).

^{1}H NMR (400 MHz, $CDCl_3$) δ = 8.60 (d, 2H), 8.22 (d, 2H), 7.76 (s, 2H), 6.07 (s, 1H), 5.52 (s, 1H), 4.59–4.49 (m, 4H), 1.88 (s, 3H).

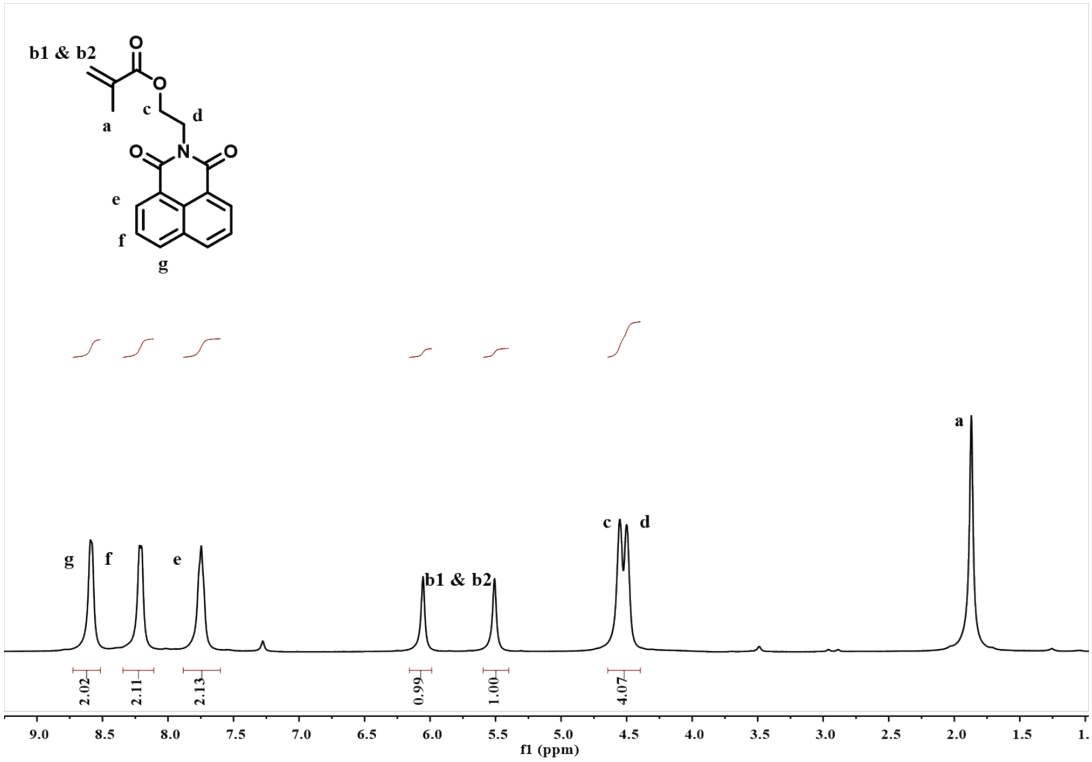

Figure S18. ^{1}H NMR (400 MHz, $CDCl_3$) spectrum of **MMA-NAI**.

Synthetic procedure of MMA-NAICl

MMA-NAICl was synthesized using a similar procedure to **MMA-NAI**. 4-Chloro-1,8-naphthalenedicarboxylic anhydride (500 mg, 2.15 mmol), 2-aminoethylmethacrylate hydrochloride (534 mg, 3.23 mmol), and triethylamine (448 µL, 3.23 mmol) were used to give **MMA-NAICl** as a yellow solid (396 mg, 54%).

^{1}H NMR (400 MHz, $CDCl_3$) δ = 8.67 (dd, 1H), 8.62 (dd, 1H), 8.51 (d, 1H), 7.96–7.78 (m, 2H), 6.04 (s, 1H), 5.50 (s, 1H), 4.64–4.39 (m, 4H), 2.03 (s, 3H).

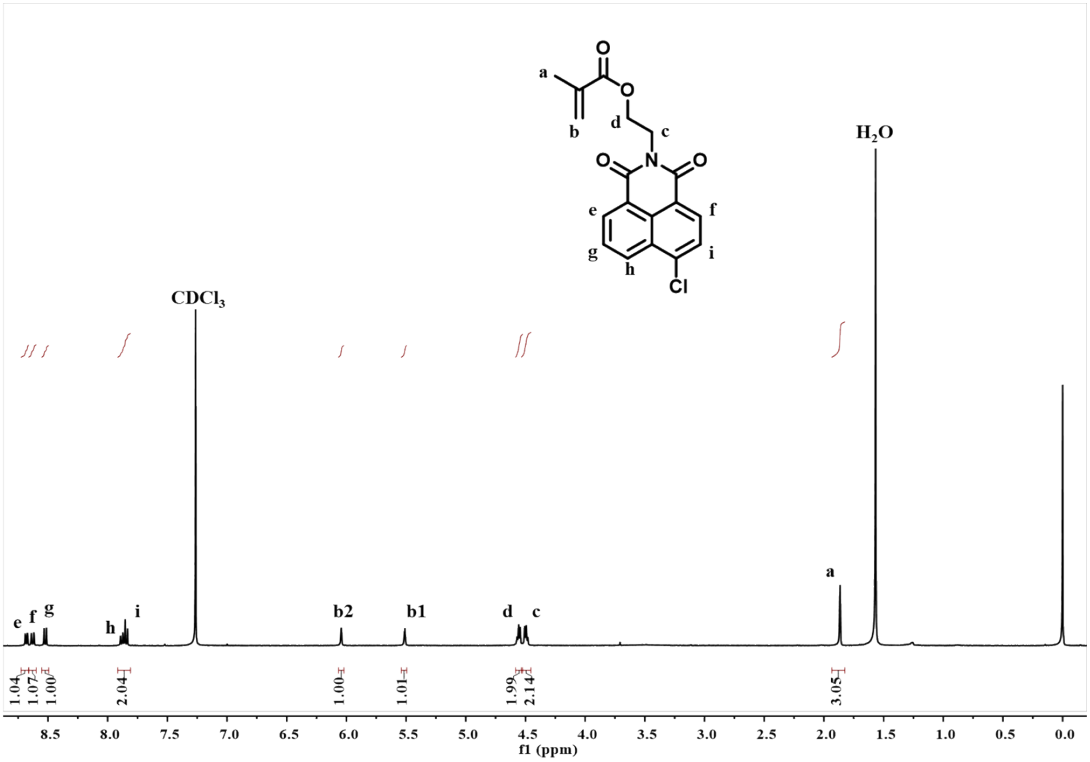

Figure S19. ^{1}H NMR (400 MHz, $CDCl_3$) spectrum of **MMA-NAICl**.

Synthetic procedure of MMA-NAIBr

MMA-NAIBr was synthesized using a similar procedure to **MMA-NAI**. 4-Bromo-1,8-naphthalenedicarboxylic anhydride (1 g, 3.6 mmol), 2-aminoethylmethacrylate hydrochloride (897 mg, 5.4 mmol), and triethylamine (752 μL, 5.4 mmol) were used to give **MMA-NAIBr** as a yellow solid (895 mg, 60%).

^{1}H NMR (400 MHz, $CDCl_3$) δ = 8.73–8.66 (m, 1H), 8.60 (dd, 1H), 8.43 (d, 1H), 8.06 (d, 1H), 7.86 (dd, 1H), 6.04 (s, 1H), 5.56–5.45 (s, 1H), 4.62–4.44 (m, 4H), 1.86 (s, 3H).

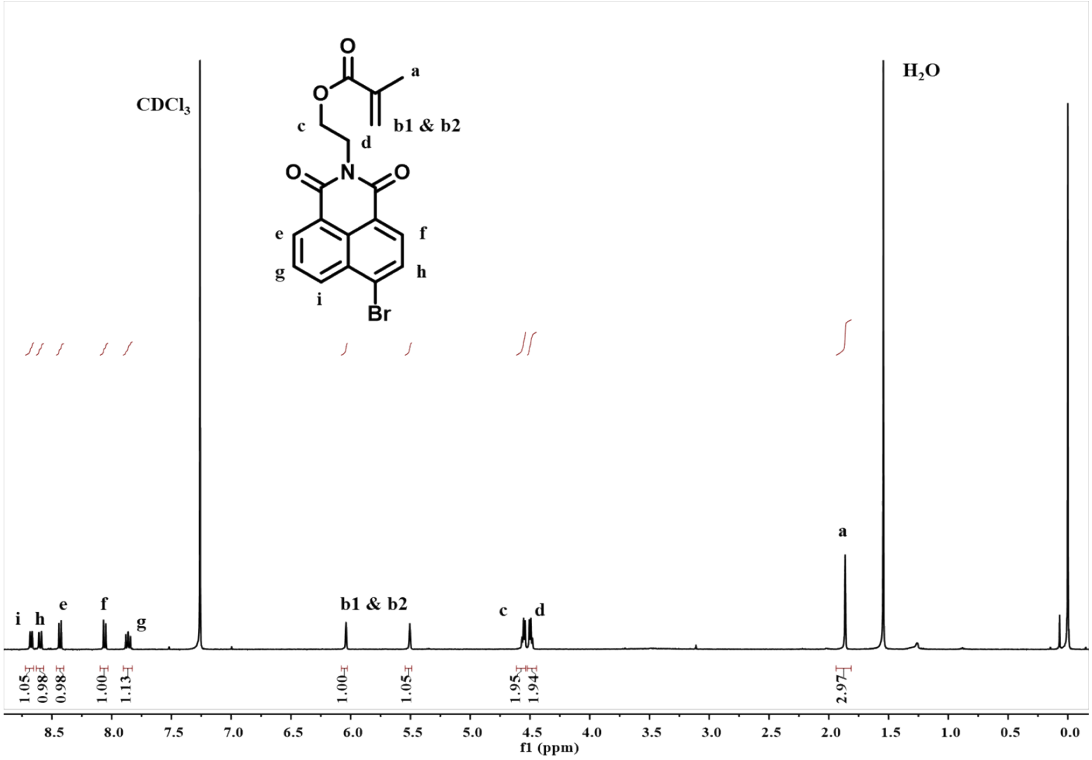

Figure S20. ^{1}H NMR (400 MHz, $CDCl_3$) spectrum of **MMA-NAIBr**.

Synthetic procedure of NAI-Boc (2)

1,8-Naphthalic anhydride (1 g, 5.05 mmol) and tert-butyl 4-aminobutanoate (1.21 g, 5.55 mmol) were dissolved in DMF (60 mL), followed by the addition of triethylamine (752 µL, 5.4 mmol). The reaction mixture was stirred at 100 °C for 16 h. After cooling to room temperature, the mixture was extracted with dichloromethane and water. The organic layers were combined, dried over anhydrous sodium sulphate, and the solvent was removed under reduced pressure. The residue was purified by column chromatography with petroleum ether and dichloromethane (10:1, v/v) as the eluent, yielding **2** as a pale-yellow solid (1.48 g, 86%).

^{1}H NMR (400 MHz, $CDCl_3$) δ = 8.63 (dd, 2H), 8.24 (dd, 2H), 7.78 (dd, 2H), 4.41–4.02 (m, 2H), 2.39 (t, 2H), 2.15–1.96 (m, 2H), 1.45 (s, 9H).

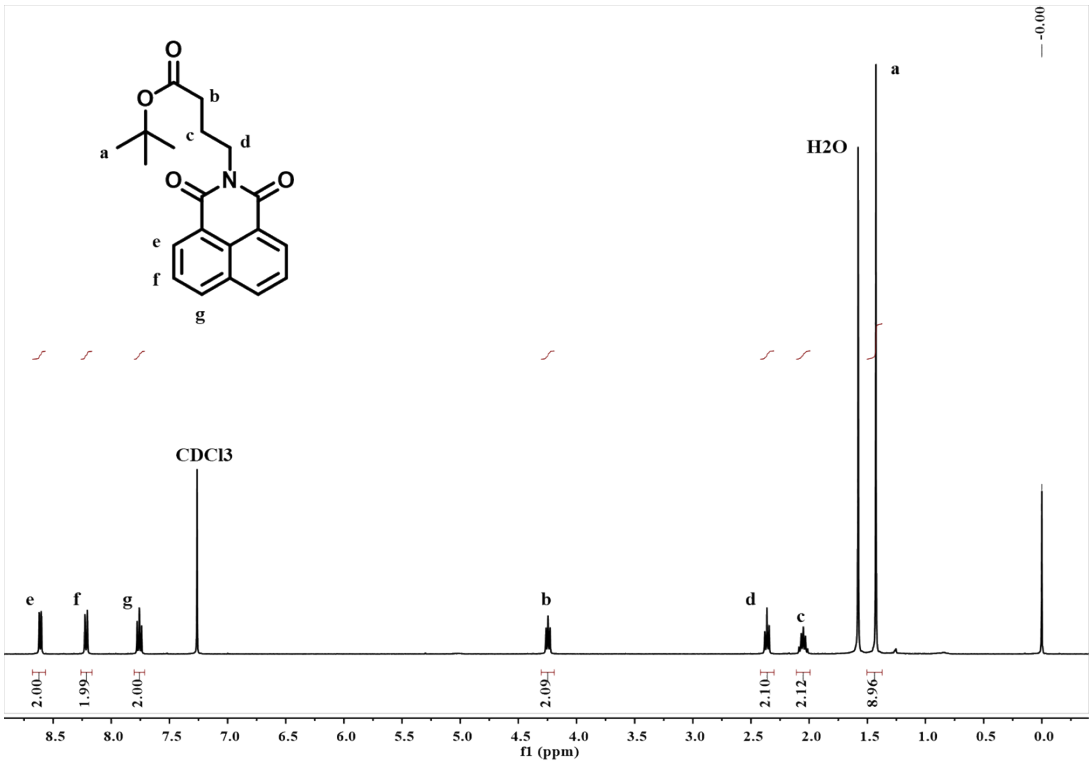

Figure S21. ^{1}H NMR (400 MHz, $CDCl_3$) spectrum of **2**.

Synthetic procedure of NAI-COOH

NAI-COOH was obtained by treating compound **2** (30 mg) with a mixture of trifluoroacetic acid (0.2 mL) and dichloromethane (0.8 mL). The solution was stirred for 4 h. After the reaction, the solvent was evaporated under a stream of nitrogen. The residue was redissolved with dichloromethane and precipitated using n-hexane, yielding **NAI-COOH** as a solid (9.9 mg, 33.0%).

^{1}H NMR (400 MHz, DMSO-d_6) δ = 12.01 (s, 1H), 8.48 (ddd, 4H), 7.88 (dd, 2H), 4.10 (t, 2H), 2.31 (t, 2H), 1.90 (t, 2H).

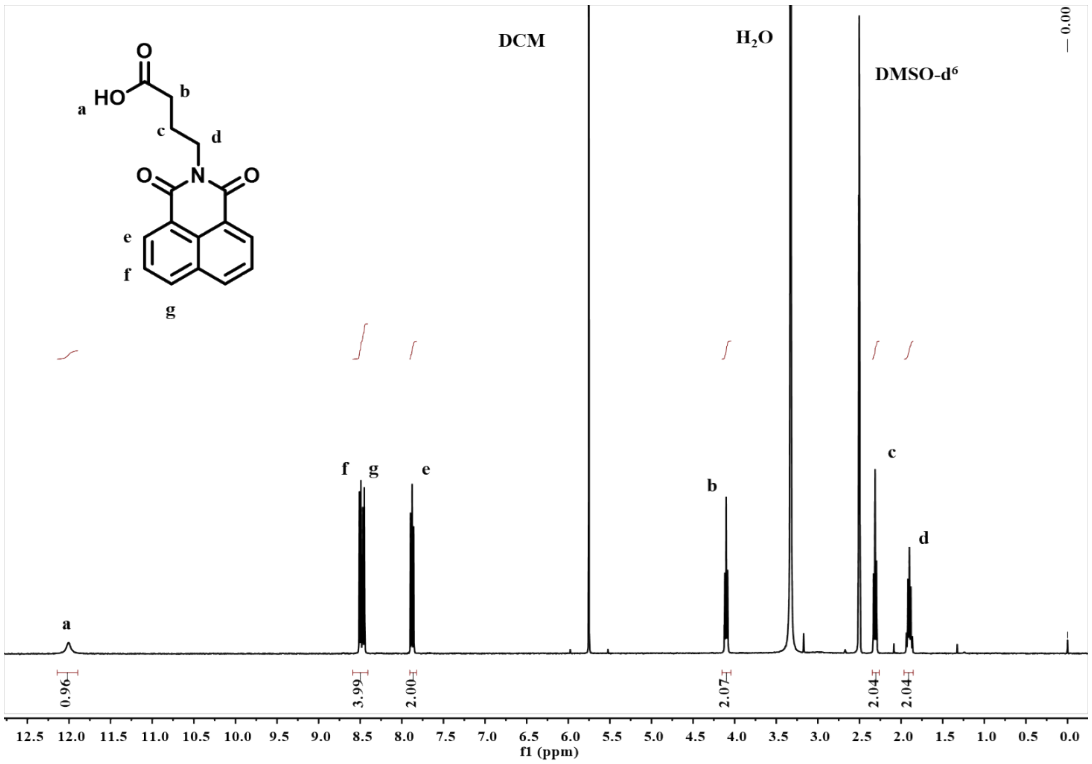

Figure S22. ^{1}H NMR (400 MHz, DMSO-d_6) spectrum of **NAI-COOH**.

Synthetic procedure of NAIBr-Boc (3)

4-bromo-1,8-naphthalenedicarboxylic anhydride (1g, 3.6 mmol) and tert-butyl 4-aminobutanoate (859 mg, 5.4 mmol) were dissolved in DMF (60 mL), followed by the addition of triethylamine (752 μL, 5.4 mmol). The reaction mixture was stirred at 100 °C for 16 h. After cooling to room temperature, the mixture was extracted with dichloromethane and water. The organic layers were combined, dried over anhydrous sodium sulphate, and the solvent was removed under reduced pressure. The residue was purified by column chromatography with petroleum ether and dichloromethane (10:1, v/v) as the eluent, yielding **3** as a yellow solid (1.14 g, 76%).

^{1}H NMR (400 MHz, $CDCl_3$) δ = 8.68 (d, 1H), 8.59 (d, 1H), 8.43 (d, 1H), 8.06 (d, 1H), 7.87 (t, 1H), 4.24 (t, 2H), 2.38 (t, 2H), 2.06 (p, 2H), 1.44 (s, 9H).

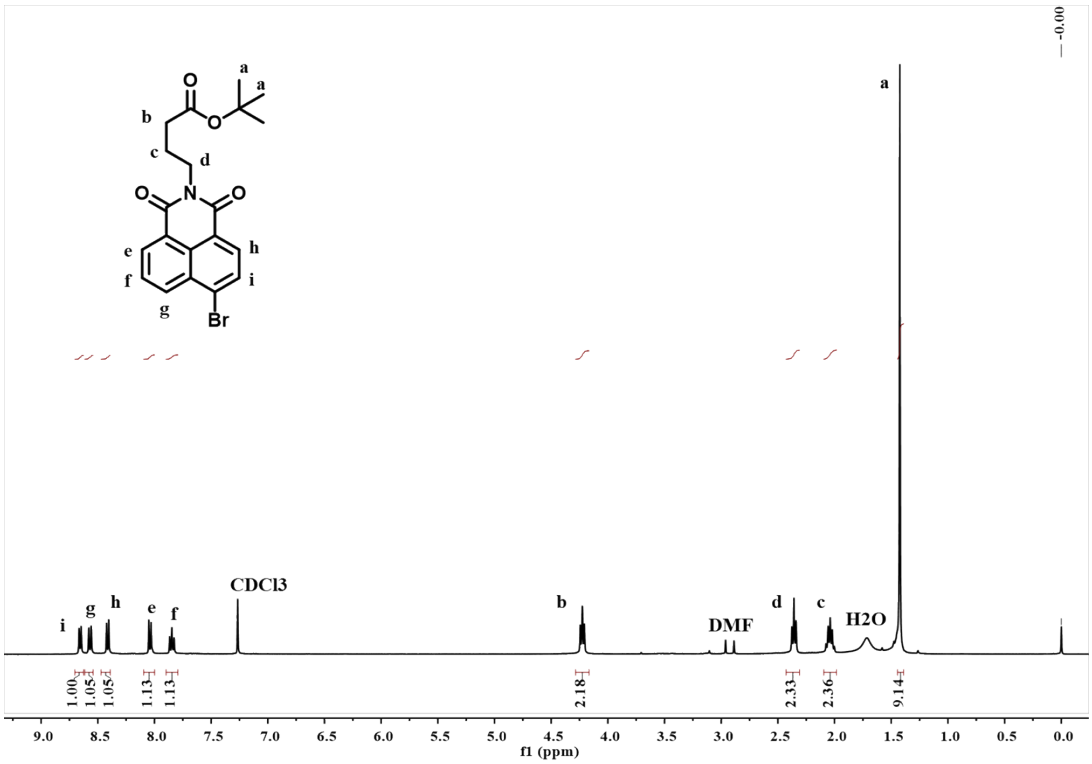

Figure S23. ^{1}H NMR (400 MHz, $CDCl_3$) spectrum of **3**.

Synthetic procedure of Ac-NAI

In a 100 mL round-bottom flask, 9,9-dimethyl-9,10-dihydroacridine (200 mg, 1.19 mmol), **NAIBr-Boc** (500 mg, 1.19 mmol), tris(dibenzylideneacetone)dipalladium (55 mg, 0.06 mmol), 1,1'-bis(diphenylphosphino)ferrocene (66 mg, 0.12 mmol), cesium carbonate (1.06 g, 3,04 mmol), and dry toluene (30 mL) were combined. The mixture was stirred at 100 °C under an argon atmosphere for 16 h. After the reaction, the solvents were evaporating under reduced pressure, and the mixture was extracted with dichloromethane (3 × 50 mL). The organic layers were successively washed with water and brine, dried over anhydrous sodium sulphate, and concentrated. The residue was purified by column chromatography with petroleum ether and dichloromethane (1:1, v/v) as the eluent, yielding **Ac-NAI** as a brown solid (314 mg, 48%).

^{1}H NMR (600 MHz, $CDCl_3$) δ = 8.82 (d, 1H), 8.64 (dd, 1H), 8.03 (dd, 1H), 7.79 (d, 1H), 7.63 (dd, 1H), 7.54 (dd, 2H), 6.95 (td, 2H), 6.86 (ddd, 2H), 5.94 (dd, 2H), 4.30 (t, 2H), 2.40 (t, 2H), 2.18–2.04 (m, 2H), 1.85 (s, 3H), 1.76 (s, 3H), 1.44 (s, 9H).

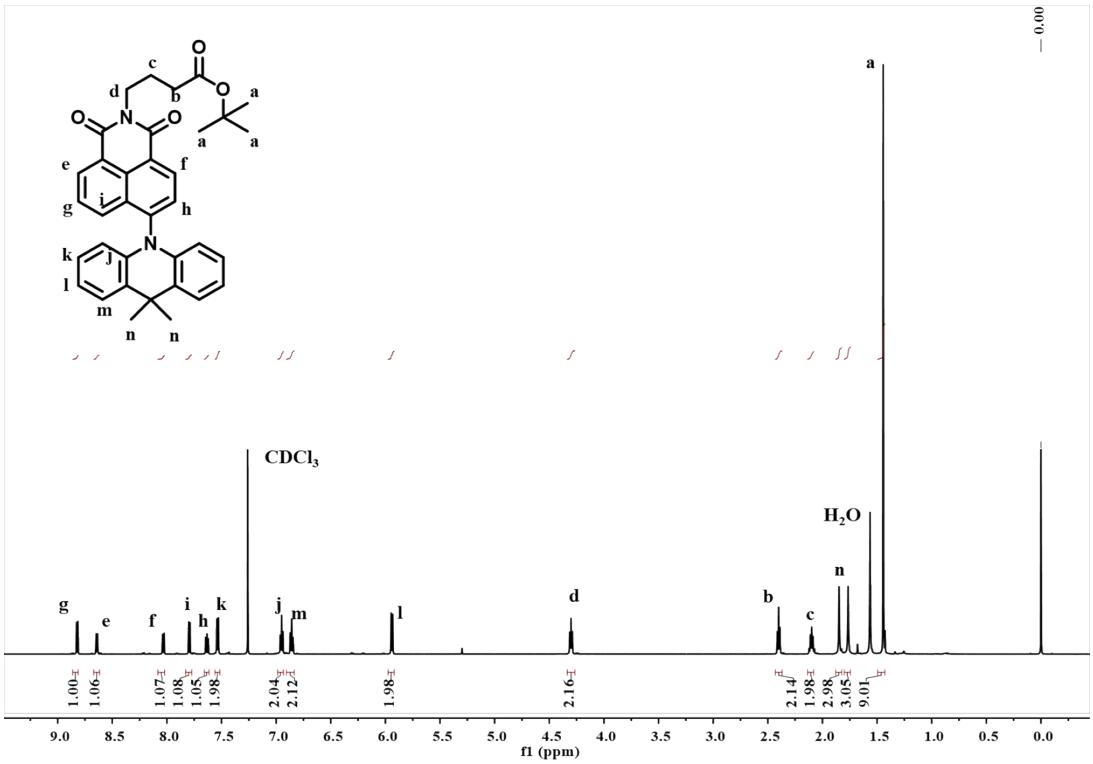

Figure S24. ^{1}H NMR (600 MHz, $CDCl_3$) spectrum of **Ac-NAI**.

General synthetic procedure of donor-acceptor copolymers

In a 4 mL vial, donor monomer and/or acceptor monomer (1 eq), V601 (0.02 eq), CTA-CN (0.1 eq) were dissolved in 1 mL of dioxane. The vial was sealed with a rubber stopper, and the reaction mixture was purged with nitrogen for 15 min to remove oxygen. The mixture was then stirred and heated to 75 °C overnight. The reaction was quenched by exposure to air. The resulting solution was precipitated in cold methanol and washed twice with methanol, yielding the D-A copolymer.

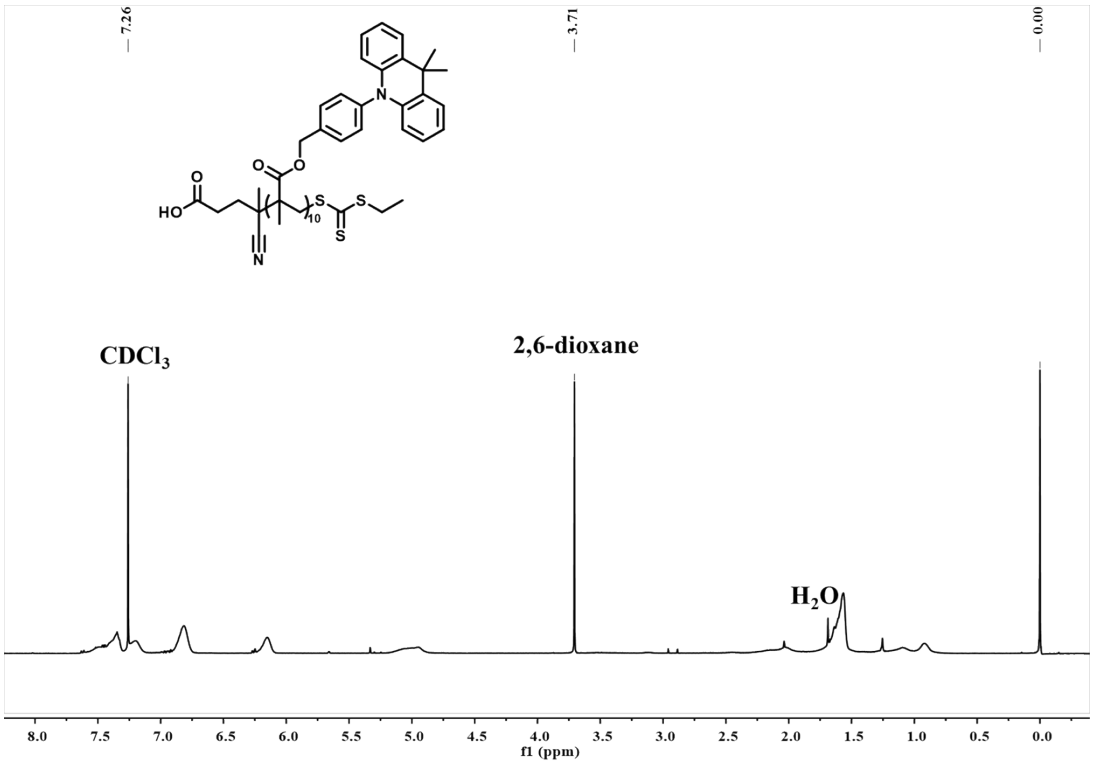

Figure S25. ^{1}H NMR (400 MHz, $CDCl_3$) spectrum of ***p*Ac$_{10}$** (white solid, 82%).

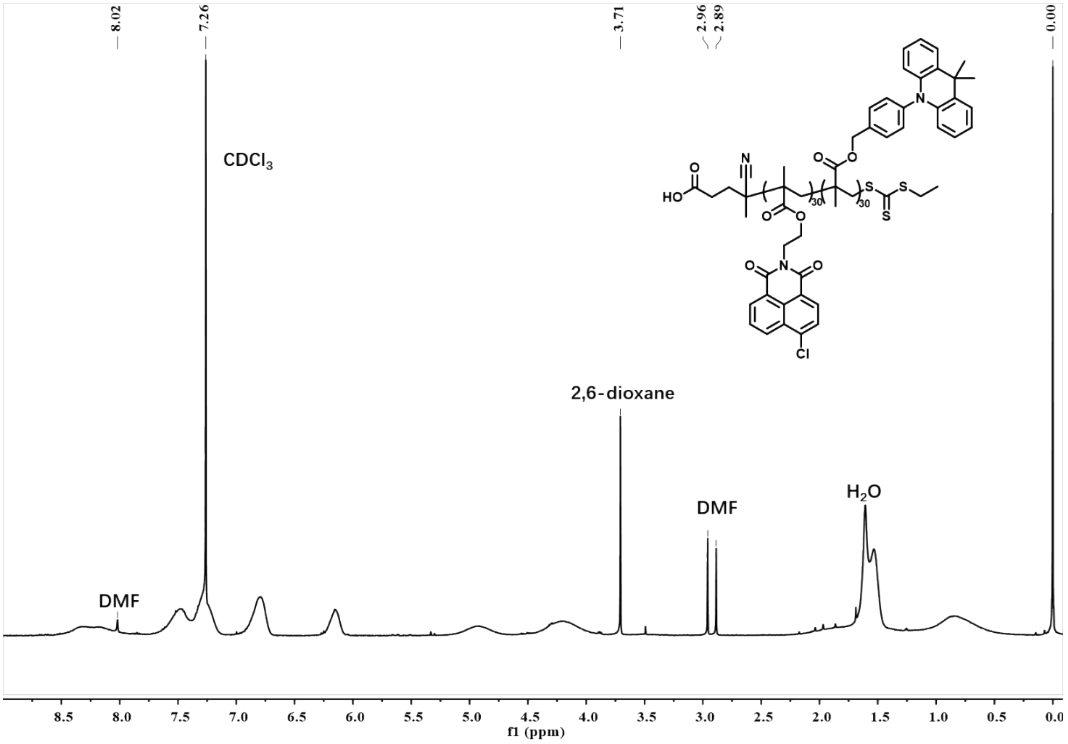

Figure S26. ^{1}H NMR (400 MHz, $CDCl_3$) spectrum of ***p*(Ac$_{30}$-*co*-NAICl$_{30}$)** (yellow solid, 98%).

MW Averages

Mp: 10633	Mn: 5745	Mv: 8710	Mw: 9173
Mz: 12233	Mz+1: 14920	PD: 1.5967	

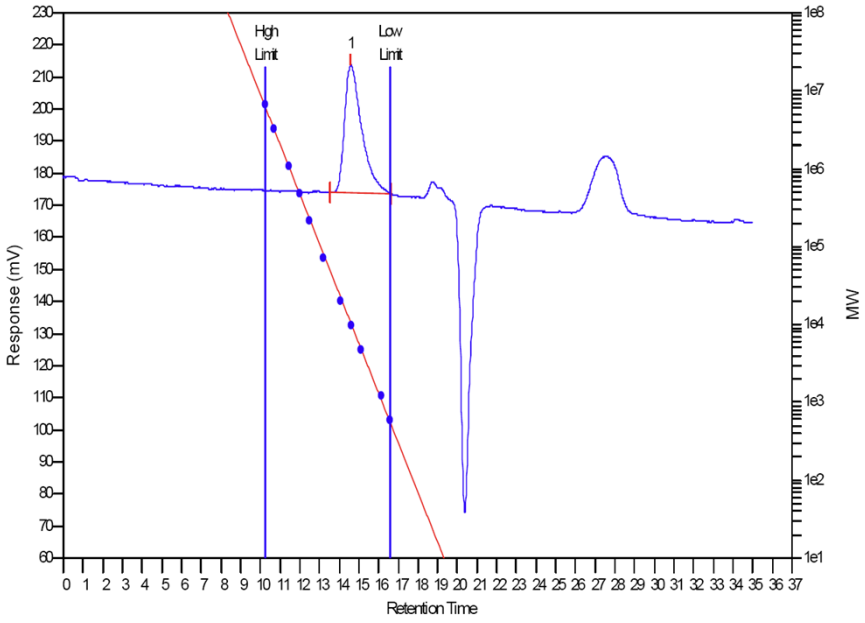

Figure S27. GPC analysis of ***p*(Ac$_{30}$-co-NAICl$_{30}$)** (1,2,4-TCB as eluent).

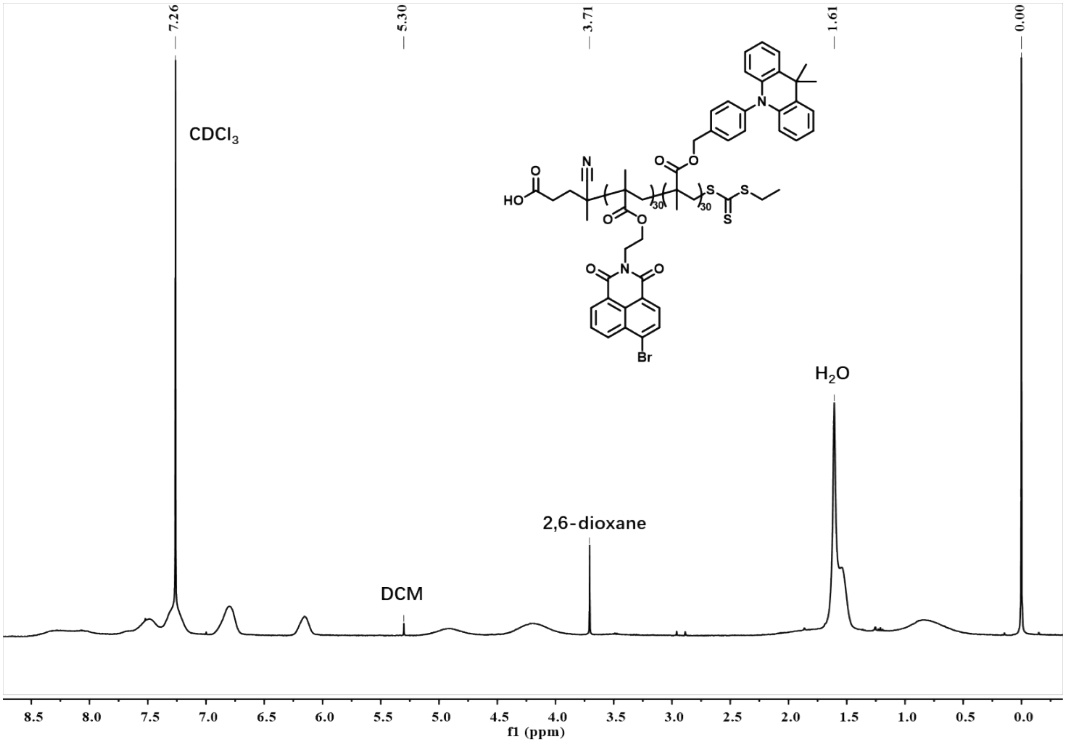

Figure S28. ^{1}H NMR (400 MHz, $CDCl_3$) spectrum of ***p*(Ac$_{30}$-co-NAIBr$_{30}$)** (yellow solid, 88%).

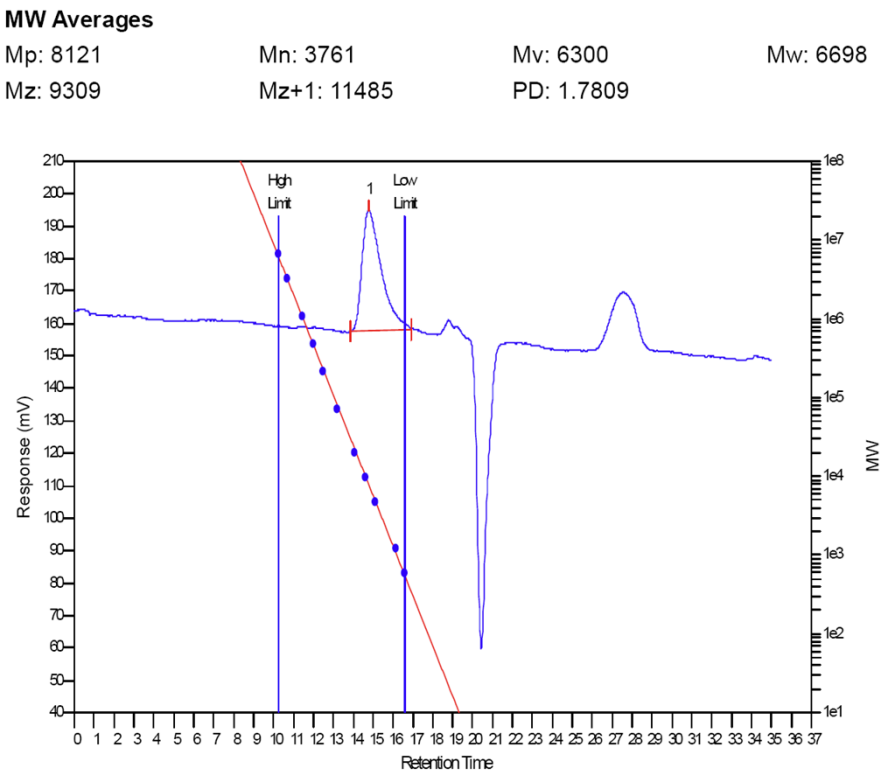

Figure S29. GPC analysis of ***p*(Ac$_{30}$-*co*-NAIBr$_{30}$)** (1,2,4-TCB as eluent).

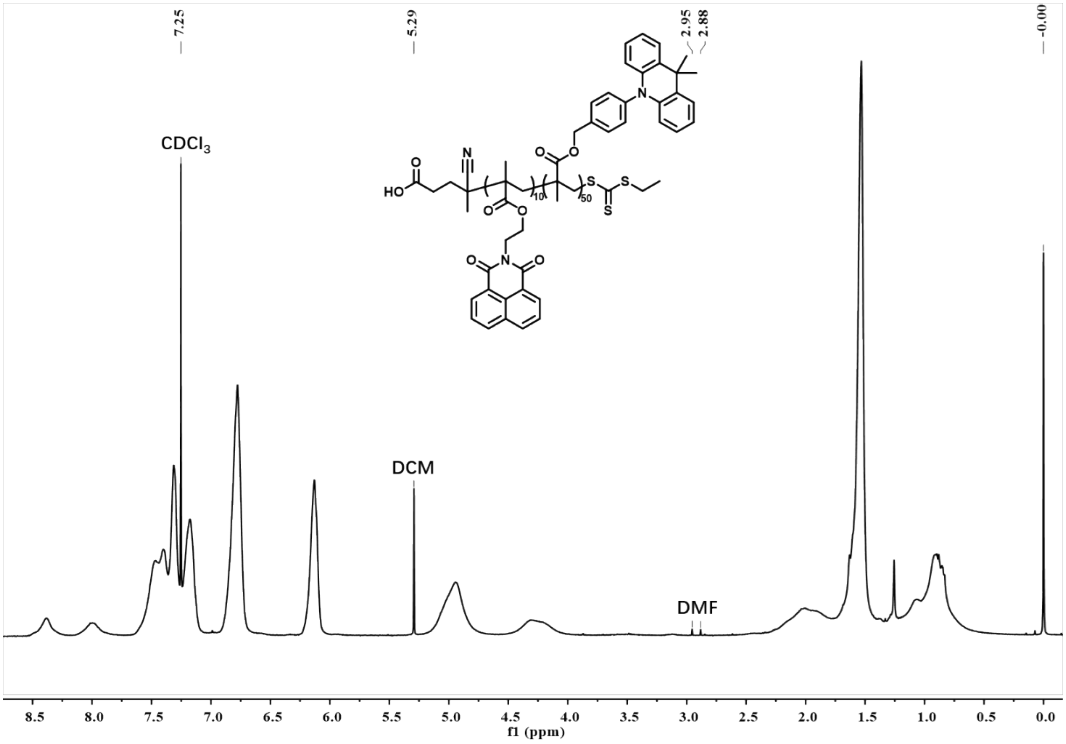

Figure S30. ^{1}H NMR (400 MHz, $CDCl_3$) spectrum of ***p*(Ac$_{50}$-*co*-NAI$_{10}$)** (yellow solid, 95%).

MW Averages

Mp: 18230	Mn: 14300	Mv: 17985	Mw: 18649
Mz: 23439	Mz+1: 28776	PD: 1.3041	

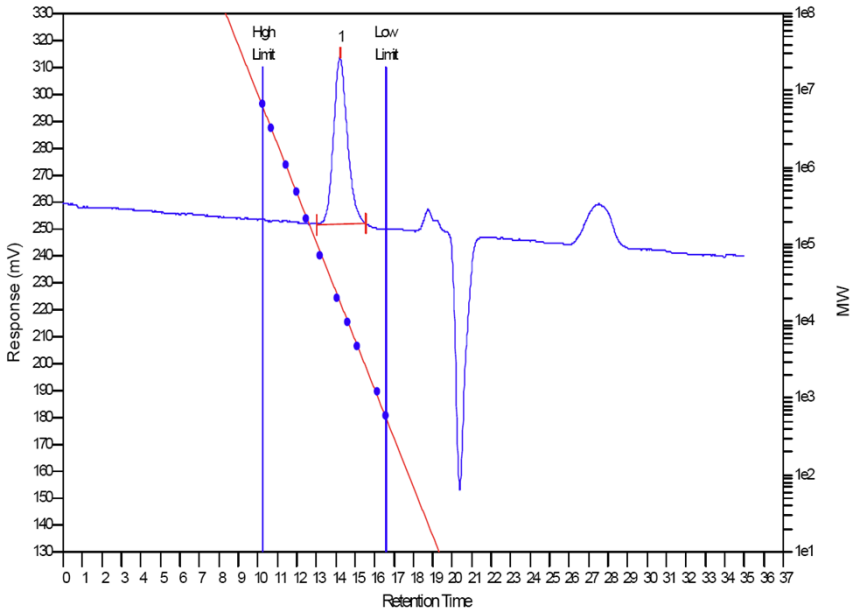

Figure S31. GPC analysis of ***p*(Ac$_{50}$-co-NAI$_{10}$)** (1,2,4-TCB as eluent).

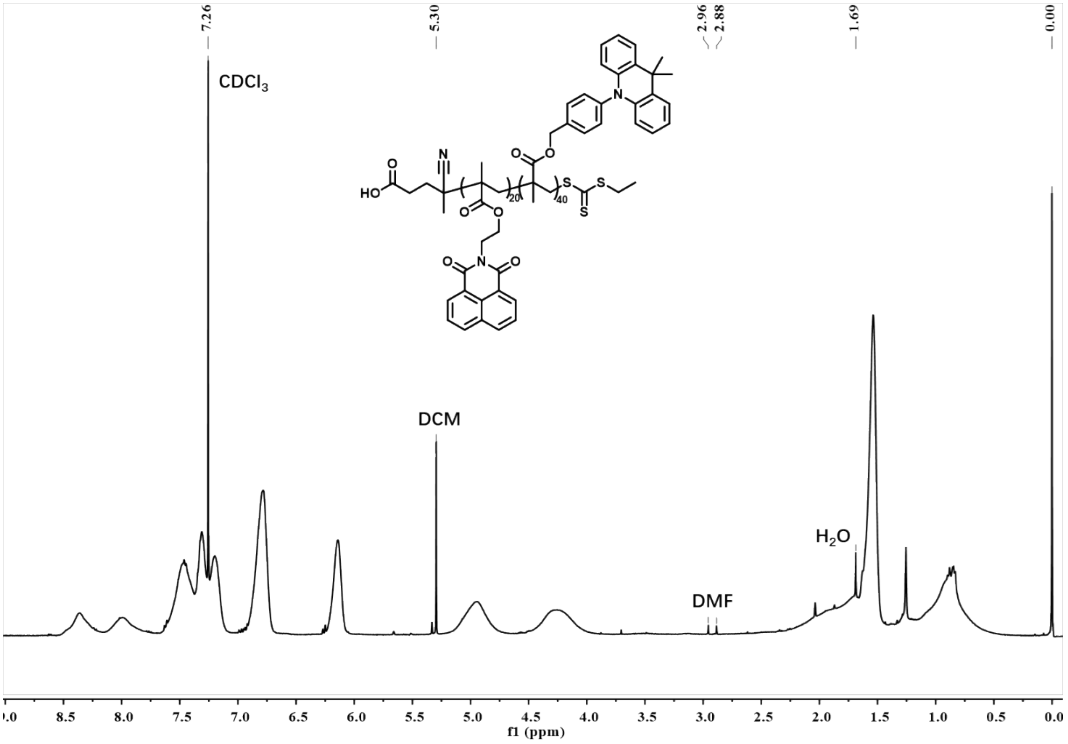

Figure S32. ^{1}H NMR (400 MHz, $CDCl_3$) spectrum of ***p*(Ac$_{40}$-co-NAI$_{20}$)** (yellow solid, 85%).

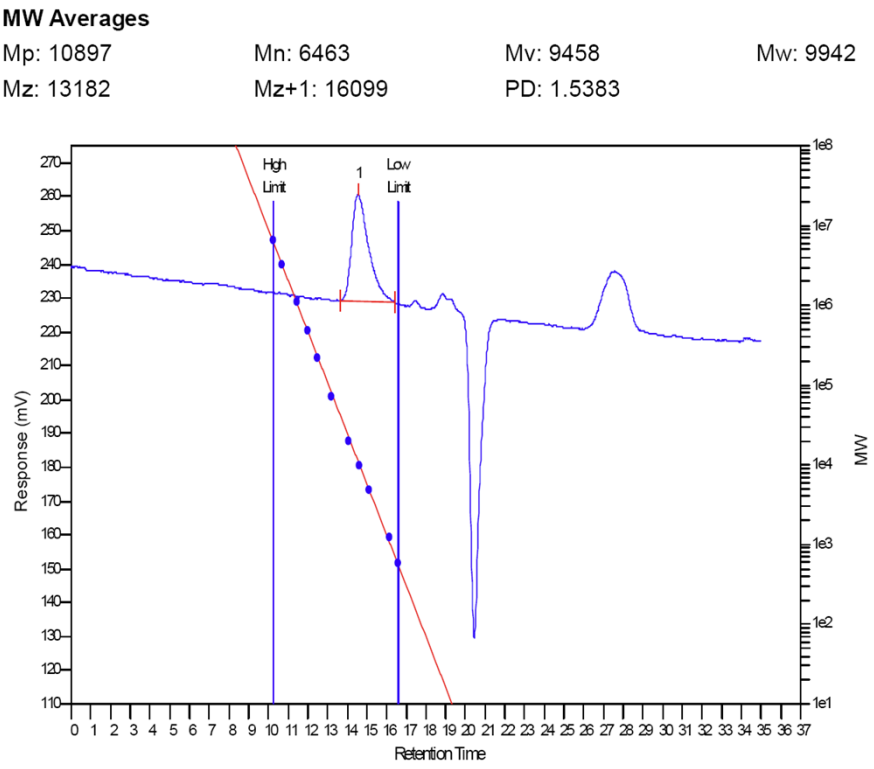

Figure S33. GPC analysis of ***p*(Ac$_{40}$-co-NAI$_{20}$)** (1,2,4-TCB as eluent).

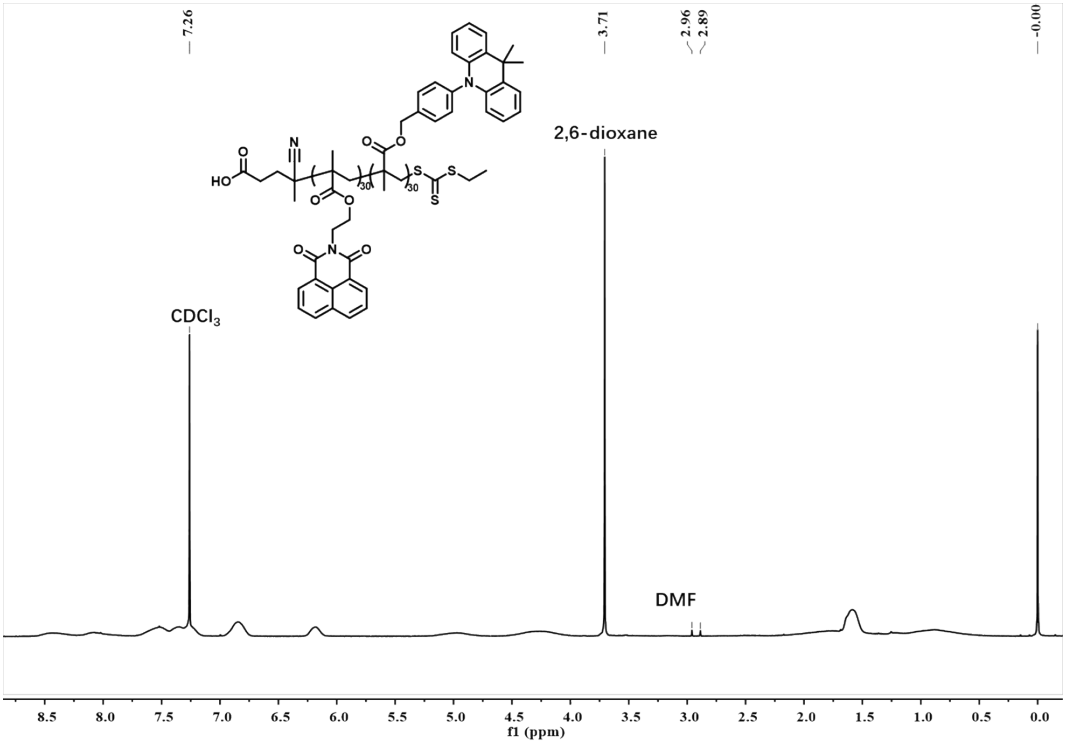

Figure S34. ^{1}H NMR (400 MHz, $CDCl_3$) spectrum of ***p*(Ac$_{30}$-co-NAI$_{30}$)** (yellow solid, 66%).

MW Averages

Mp: 4190	Mn: 2577	Mv: 3671	Mw: 3872
Mz: 5245	Mz+1: 6412	PD: 1.5025	

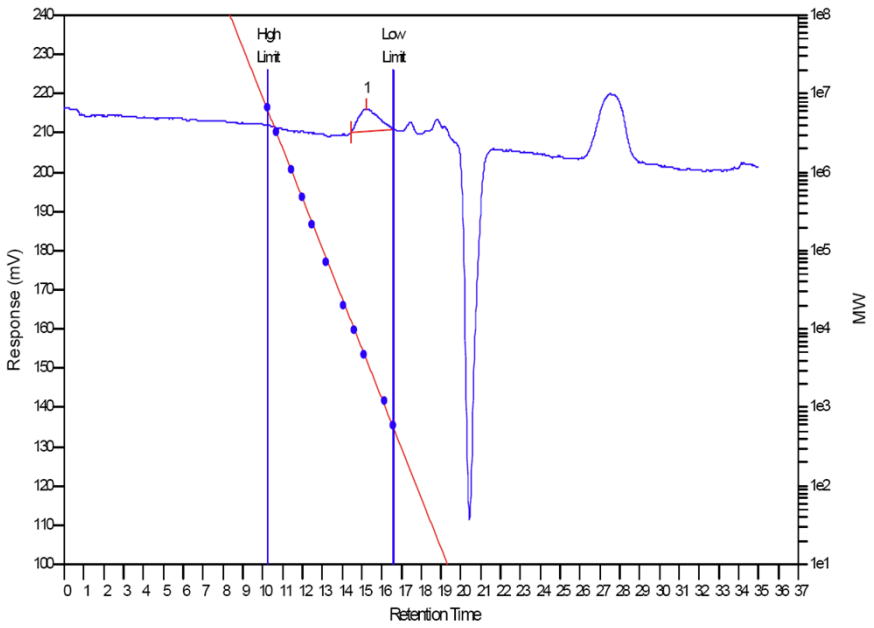

Figure S35. GPC analysis of ***p*(Ac$_{30}$-co-NAI$_{30}$)** (1,2,4-TCB as eluent).

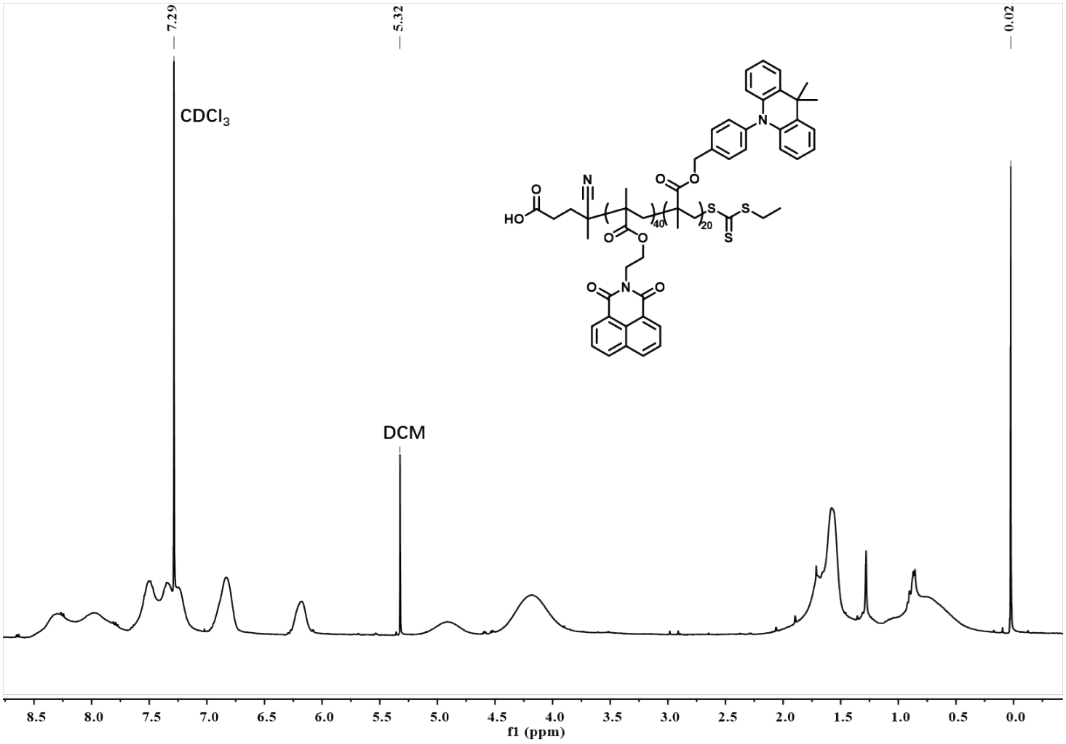

Figure S36. ^{1}H NMR (400 MHz, $CDCl_3$) spectrum of ***p*(Ac$_{20}$-co-NAI$_{40}$)** (yellow solid, 62%).

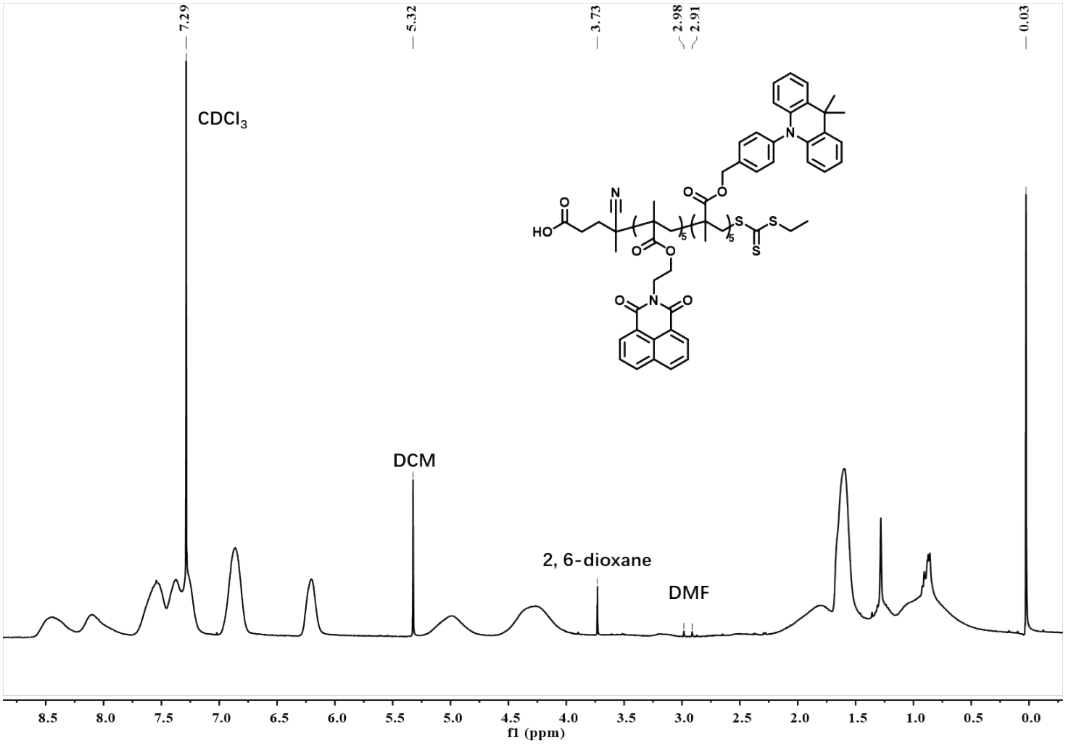

Figure S37. ^{1}H NMR (400 MHz, $CDCl_3$) spectrum of ***p*(Ac$_5$-co-NAI$_5$)** (yellow solid, 100%).

General synthetic procedure of amphiphilic polymers

N, *N*-Dimethylacrylamide (60 eq), macro-CTA (hydrophobic polymer block) (1 eq), and V601 (0.02 eq) were added to a vial containing 1000 μL of dioxane and equipped with a magnetic stir bar. The mixture was deoxygenated by bubbling nitrogen through the solution for 15 min. The reaction was initiated by immersing the vial in a 70 °C oil bath and maintained for 20 h. After the reaction, the solution was precipitated with diethyl ether to obtain the product.

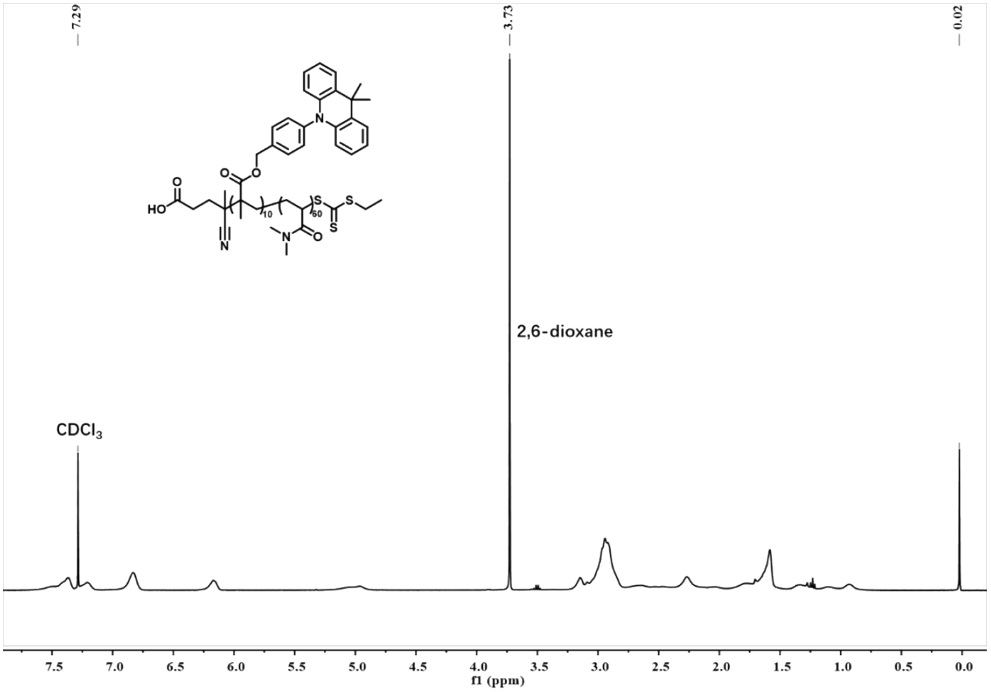

Figure S38. ^{1}H NMR (400 MHz, $CDCl_3$) spectrum of ***p*Ac$_{10}$-*b*-*p*DMA$_{60}$** (yellow solid, 99%).

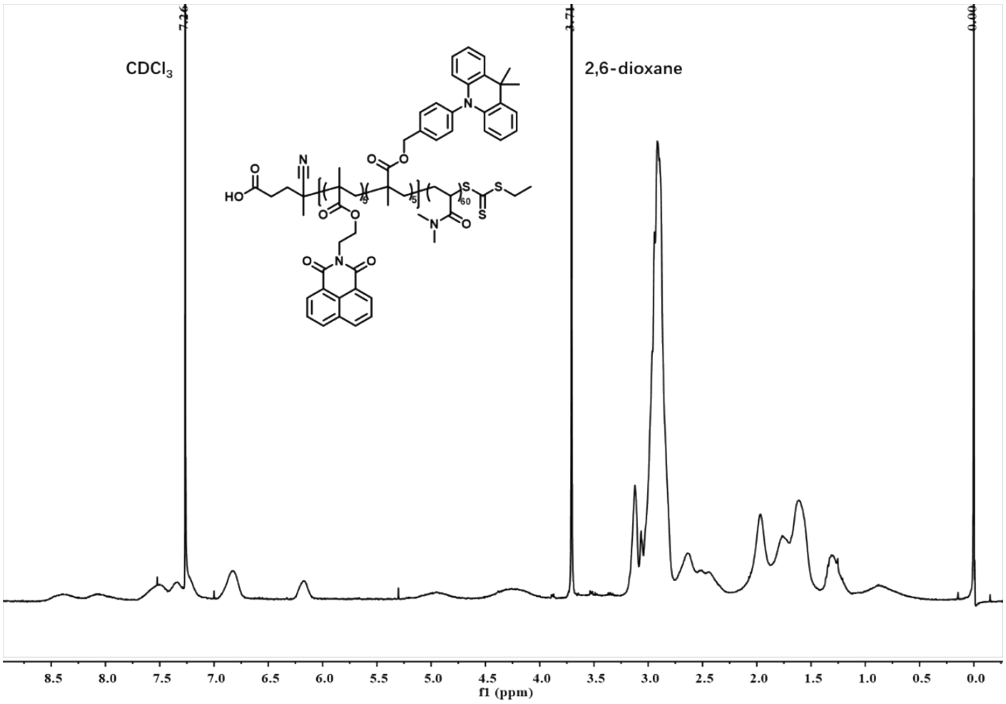

Figure S39. ^{1}H NMR (400 MHz, $CDCl_3$) spectrum of ***p*[Ac$_5$-co-NAI$_5$]-*b*-*p*DMA$_{60}$** (yellow solid, 99%).

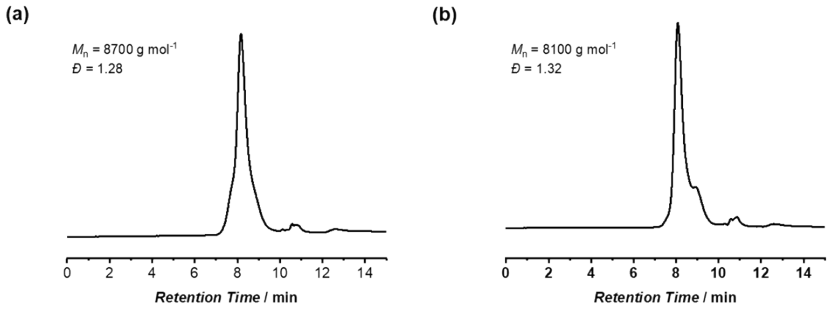

Figure S40. GPC analysis of ***p*Ac$_{10}$-*b*-*p*DMA$_{60}$** (a) and ***p*[Ac$_5$-co-NAI$_5$]-*b*-*p*DMA$_{60}$** (b) (THF as eluent).

General synthetic procedure of cyclic peptide-based supramolecular units

Cyclic peptide (1 eq) and carboxyl compound (1.5 eq) were dissolved in DMF. To this solution, HATU (1.5 eq) and NMM (3 eq) were added. The reaction mixture was allowed to proceed for 24 h. After completion, the DMF solution was precipitated into a mixed solvent of dichloromethane and diethyl ether, in which the carboxyl compound is soluble. This process yielded the cyclic peptide-based supramolecular unit.

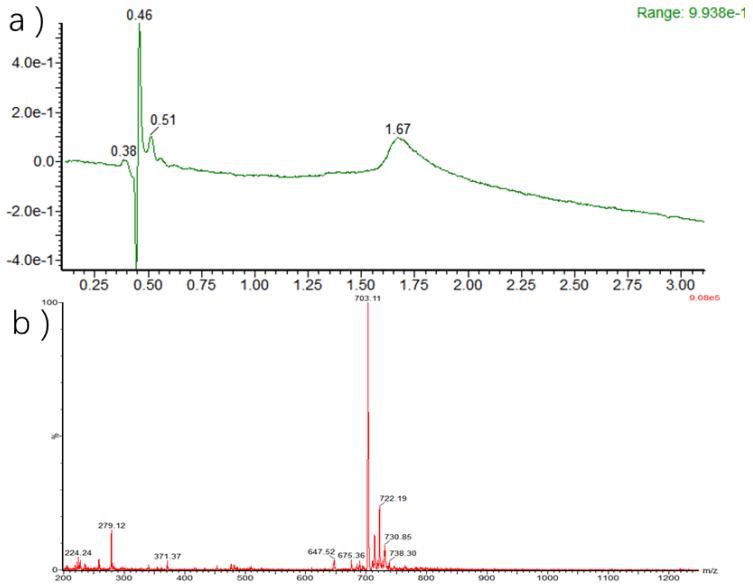

Figure S41. LC-MS analysis of **CP-NAI** (a) LC profile using UV detector; (b) mass spectrum of the LC peak (m/z=703.1, $[C_{79}H_{97}N_{13}O_{11}]^{2+}$:702.9).

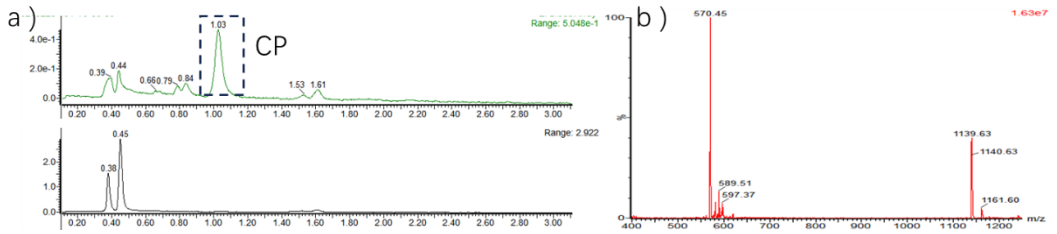

Figure S42. LC-MS analysis of **CP-*p*Ac$_{10}$-*b*-*p*DMA$_{60}$** reaction (a) LC profile of t_0 & t_1 using UV detector, indicating that the conversion is up to 99%; (b) mass spectrum of CP peak in the LC profile (m/z=1139.6, $[C_{63}H_{87}N_{12}O_8]^+$: 1139.7).

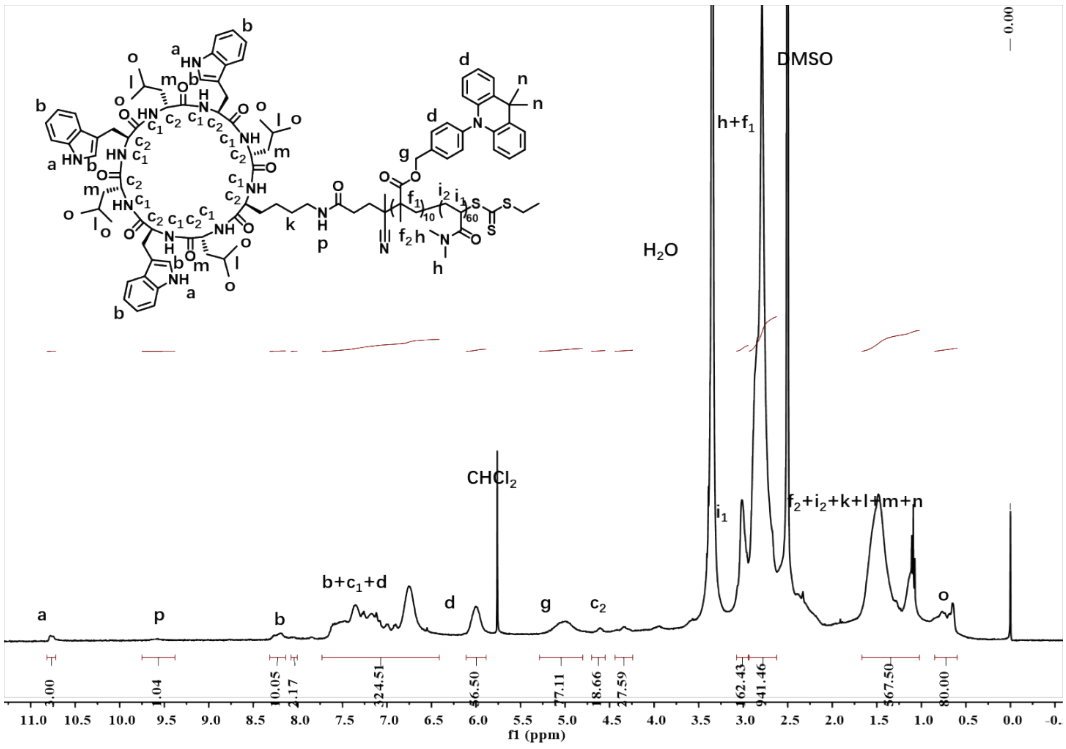

Figure S43. ^{1}H NMR (400 MHz, DMSO-d_6) spectrum of **CP-*p*Ac$_{10}$-*b*-*p*DMA$_{60}$**.

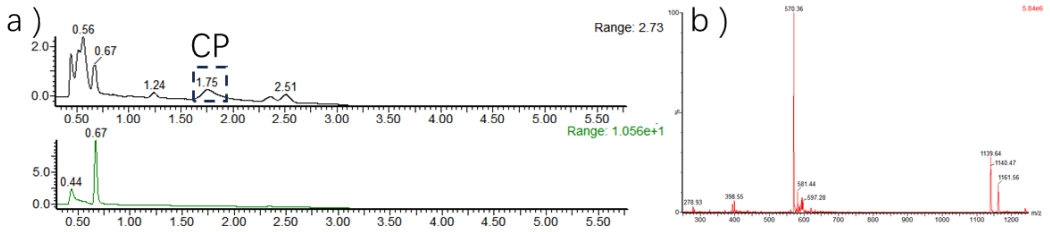

Figure S44. LC-MS analysis of **CP-*p*[Ac$_5$-*co*-NAI$_5$]-*b*-*p*DMA$_{60}$** reaction (a) LC profile of t_0 & t_1 using UV detector, indicating that the conversion is up to 99%; (b) mass spectrum of CP peak in the LC profile (m/z=1139.6, $[C_{63}H_{87}N_{12}O_8]^+$: 1139.7).

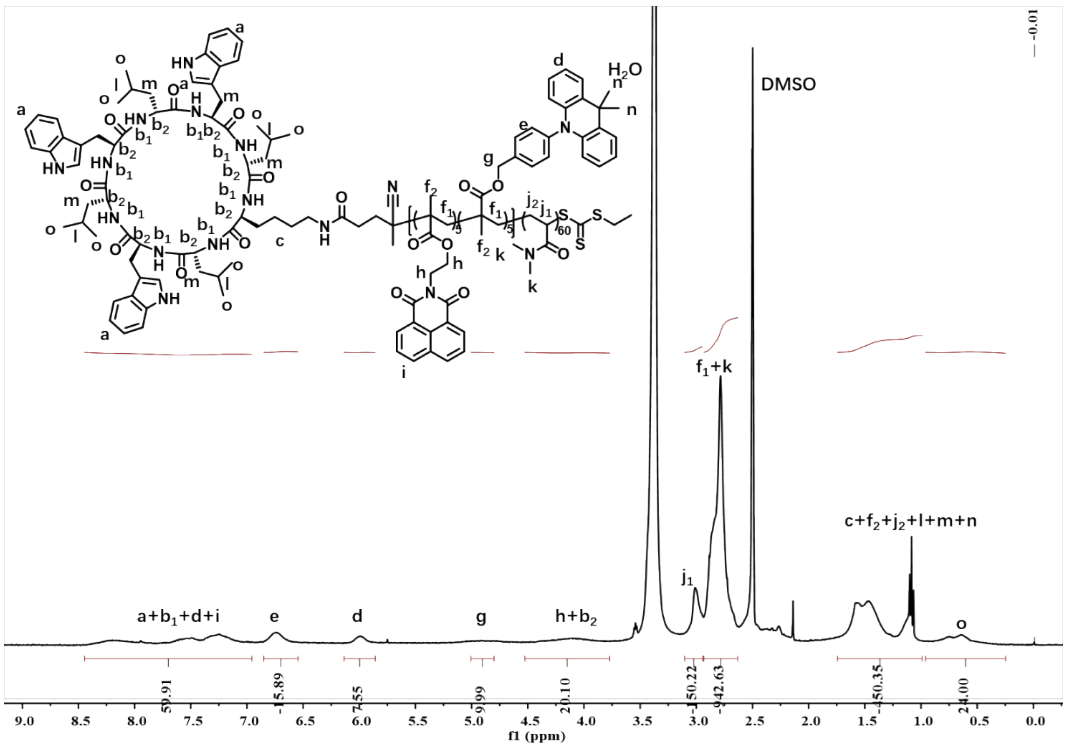

Figure S45. ^{1}H NMR (400 MHz, DMSO-d_6) spectrum of **CP-*p*[Ac$_5$-co-NAI$_5$]-*b*-*p*DMA$_{60}$**.

S5. References

1. H. Lu, Y. Wang, S. K. Hill, H. Jiang, Y. Ke, S. Huang, D. Zheng, S. Perrier and Q. Song, *Angew. Chem. Int. Ed.*, 2023, **62**, e202311224..
2. Y. Hu, J. Miao, T. Hua, Z. Huang, Y. Qi, Y. Zou, Y. Qiu, H. Xia, H. Liu, X. Cao and C. Yang, *Nat. Photonics*, 2022, **16**, 803-830.
3. J. Huo, S. Xiao, Y. Wu, M. Li, H. Tong, H. Shi, D. Ma and B. Tang, *Chem. Eng. J.*, 2023, **452**, 138957.
4. J. Deckers, T. Cardeynaels, H. Penxten, A. Ethirajan, M. Ameloot, M. Kruk, B. Champagne and W. Maes, *Chem.-Eur. J.*, 2020, **26**, 15212-15225.
5. S. Shao, J. Hu, X. Wang, L. Wang, X. Jing and F. Wang, *J. Am. Chem. Soc.*, 2017, **139**, 17739-17742.
6. Z. Li, W. Chen, J. Hale, C. Lynch, S. G. Mills, R. Hajdu, C. A. Keohane, M. J. Rosenbach, J. A. Milligan, G. J. Shei, G. Chrebet, S. A. Parent, J. Bergstrom, D. Card, M. Forrest, E. J. Quackenbush, L. A. Wickham, H. Vargas, R. M. Evans, H. Rosen and S. Mandala, *J. Med. Chem.*, 2005, **48**, 6169-6173.